R-92-XX

TRACTIVE SHEAR TESTS OF RIVERBED CLAY SAMPLES OBTAINED DOWNSTREAM OF COULEE DAM

Month 1992

U.S. DEPARTMENT OF THE INTERIOR
Bureau of Reclamation
Denver Office
Research and Laboratory Services Division
Hydraulics Branch

7-2090 (4-81)
Bureau of Reclamation

TECHNICAL REPORT STANDARD TITLE PAGE

1. REPORT NO. R-92-XX	2. GOVERNMENT ACCESSION NO.	3. RECIPIENT'S CATALOG NO.
4. TITLE AND SUBTITLE TRACTIVE SHEAR TESTS OF RIVERBED CLAY SAMPLES OBTAINED DOWNSTREAM OF COULEE DAM		5. REPORT DATE Month 1992 6. PERFORMING ORGANIZATION CODE D-3751
7. AUTHOR(S) R. A. Dodge		8. PERFORMING ORGANIZATION REPORT NO. R-92-XX
9. PERFORMING ORGANIZATION NAME AND ADDRESS Bureau of Reclamation Denver Office Denver CO 80225		10. WORK UNIT NO. 11. CONTRACT OR GRANT NO. 13. TYPE OF REPORT AND PERIOD COVERED
12. SPONSORING AGENCY NAME AND ADDRESS Same		14. SPONSORING AGENCY CODE DIBR

15. SUPPLEMENTARY NOTES

Microfiche and hard copy available at the Denver Office, Denver, Colorado.

16. ABSTRACT

Clay riverbed samples downstream of the Third Coulee Powerplant were tested in a rectangular duct-type tractive shear testing device in the Bureau of Reclamation Hydraulic Laboratory. Reclamation divers developed techniques for bringing up 0.3- by 0.3- by 0.15-meter (12- by 12- by 6-inch) samples. Several modes of scour were observed and described. Values of tractive shear for when erosion was first noted were obtained. Concepts and theory are discussed, pointing out problems and limitations of tractive shear determinations using test devices. Although neither exact incipient transport tractive shear values nor rates of erosion could be determined, the studies provided much insight into modes of erosion and increased the capability of estimating areal extent of erosion with respect to river discharge. A design curve is presented for determining diameter for gravel blanket side-bank slopes to protect exposed clay.

17. KEY WORDS AND DOCUMENT ANALYSIS

a. DESCRIPTORS-- erosion resistance/ tractive shear/ clay/ silty clay/ bedded clay/ jointed/ scour

shear test device/

b. IDENTIFIERS--

c. COSATI Field/Group COWRR: SRIM:

18. DISTRIBUTION STATEMENT	19. SECURITY CLASS (THIS REPORT)	21. NO. OF PAGES
Available from the National Technical Information Service, Operations Division, 5285 Port Royal Road, Springfield, Virginia 22161.	UNCLASSIFIED	
	20. SECURITY CLASS (THIS PAGE) UNCLASSIFIED	22. PRICE

R-92-XX

TRACTIVE SHEAR TESTS OF RIVERBED CLAY SAMPLES OBTAINED DOWNSTREAM OF COULEE DAM

by

R. A. Dodge

Hydraulics Branch
Research and Laboratory Services Division
Denver Office
Denver, Colorado

Month 1992

UNITED STATES DEPARTMENT OF THE INTERIOR ★ BUREAU OF RECLAMATION

ACKNOWLEDGMENTS

Field personnel helped prepare for and conduct the erosion tests. Steve Saure did the final design and drawings for the project shops using conceptual drawings provided by the Hydraulics Branch, Denver Office. The regional diving team developed the techniques used to bring up the clay samples. Brent Carter took preliminary diving notes and made geological observations of the samples (see appendix) in place and just after they were brought up from the river bottom. Randy Harris made further preliminary observations before, during, and after the erosion testing (appendix). Rod Rederick and Stan Yiral trimmed and placed the clay samples in the test duct and supervised and/or performed standard clay soil properties tests of the samples. Project pipefitters installed the test duct and operated the valves during the erosion tests. They also reinstalled the valves after failure of rubber seats and seals. Project machinists repaired and modified the sample lifting and leveling system. The expertise and help from these and other field personnel were greatly appreciated during a tight ongoing project construction and inspection schedule. Lee Elgin, Denver Office, organized and prepared the instrumentation for calibrating the pressure cells used for pitot velocity measurements.

CONTENTS

Page

TABLES

Table

CONTENTS - Continued

FIGURES

GLOSSARY

α Angle of flow relative to horizontal line in plane of canal bank

A Area

b Boundary or characteristic

C_p Gessler fully developed flow shear values

%C Percent clay

c Critical flow condition

d_{50} Mean grain size

d Diameter of grain

C_s Compressive strength

D Depth of flow

Δ Infinitesimal difference

e Voids ratio

E_r Erosion resistance parameter (undefined)

F Froude number $V = \sqrt{gD}$

f Weisbach friction factor

g Acceleration, also used as subscript to denote gravity effect

γ Specific weight

h_l Head loss

I_t Intensity of turbulence

K_s Rugosity

K Constants

μ Viscosity

L Reach length

LL Liquid limit

P Wetted perimeter

PI Plasticity index

PL Plastic limit

p Probability

Φ Function of

ϕ Bank slope

R Hydraulic radius

r Rate

ρ Density

S Slope

s Sediment

S_{vs} Vane shear

T Tractive shear

t Transport threshold

U* Shear velocity

V Velocity

w Water

X Distance along flow bed

Z Elevation of flow bed

Z Slope horizontal to 1

PURPOSE AND APPLICATION

This report describes the background for the design of a duct-type tractive shear test device, records experience with the device, and describes the results of tests done on several bedded clay samples taken from the river bottom. Some recommendations are made for improving tractive shear test devices, test procedures, and analyses. Limitations of shear test devices and application of critical shear values determined with them to actual riverflow are discussed. Results of this study can be applied to future clay erosion studies.

INTRODUCTION

Some of the banks of the river downstream of Grand Coulee (Dam??) are naturally unstable and subject to sliding failures. Snowmelt, wet weather, and river water surface drawdown have been suspected to contribute to initiating and aggravating sliding. Because of the combined effects of operation of Chief Joseph Dam and possible shutdown during peaking operation of 10 units of the Third Coulee Powerplant followed by pumping, changes in water surface up to about 10.7 m (35 ft) are possible. Each generator unit releases about 878 m^3/s (31 000 ft^3/s) to flow downriver at maximum load. If the old powerplants and new units are operated at maximum capacity, they will produce a total of about 11 500 m^3/s (405 000 ft^3/s) of downriver flow.

A 1:120 scale physical model (fig. 1) helped determine the effects of the Third Powerplant discharges on bank stability. This study was used to determine local tractive shear values on the riverbed and provide means to determine the size rock that would not move when exposed to model-determined tractive shear values.

Based on tractive force values measured on the river bottom in the 1:120 model, clay deposits (which were not at the location of maximum tractive force) could be protected with 102-mm (4-in) diameter gravel blankets with the exception of STA 58+22 (Sta. 191+00), which would require a blanket of 305-mm (12-in) boulders to prevent erosion. If for some reason the maximum shear at this station moved to the left side over the clay, a blanket of 508-mm (20-in) boulders would be required. It was recommended that the right bank from STA 52+12 to STA 59+44 (Sta. 171+00 to Sta. 195+00) be aligned at least according to the original specifications. After alignment, the maximum tractive force would probably be no greater than 100 Pa (2.1 lb/ft^2). On the flat river bottom, 254-mm (10-in) diameter material would be sufficient to protect the clay against 11 461-m^3/s (405 000-ft^3/s) flow.

Some clay exposures in the river near toes of known slide areas still concerned the designers. It was estimated that about 1 percent of the physically modeled riverbed is exposed clay. There were some reports that moss was growing on some of the clay and, therefore, some thought that the clay may not be moving. However, these growths could be seasonal and occur between periods of high flow and scour. Diver photographs showed one example (fig. 2) of platelet deposits that were eroded and transported about 305 m (1,000 ft) downriver. A Pacific Northwest Regional dive team report, February 1981, described observations of clay erosion relative to reference pins in the river bottom. They recorded 0.015 to 0.15 m (0.05 to 0.5 ft) of erosion during 1 to 3 years of observation.

Regional and project geologists were told the 1:120 physical model could not scale predict clay erosion, but samples could be shipped to our Denver laboratories and subjected to flows and observed. The geologists strongly suggested that, rather than shipping fragile bedded clay samples to the Denver Office, a device be built at the project for testing samples with actual river water. Later, the project geologist requested that the Hydraulics Branch provide conceptual design drawings for the device and personnel to help conduct the tests.

Regional divers brought up practice samples and developed techniques for obtaining test samples. After project shop pipefitters finished fabricating and installing the test facility, divers brought up the several samples which were tested during October 1981.

CONCLUSIONS

1. The sampling techniques developed by the division team and the plastic sample container boxes made by the Denver Office Laboratory Shops were successful in obtaining the clay samples.

2. Most samples were adequate for testing following submerged storage in plastic containers for 1-1/2 to 4 weeks. However, the natural flow surface of one sample stuck to the bottom of the plastic box and separated when the sample was removed. Outer layers and edges of silty clay became mushy. The top layer of a fat clay sample bent and parted because differential drying of its adjacent layer occurred during the trimming process.

3. Only one natural flow surface was tested because the effects mentioned in conclusion 2, combined with other handling and existing joint parting, required the cutting of most samples to more intact surfaces for erosion testing.

4. No adequate material was found for sealing between the clay samples and the sample receiver. The best procedure was to wedge the samples into contact with the upstream edge of the sample receiver and fill the spaces with a clay and cement mixture.

5. Four-point leveling, rather than three-point leveling, would have provided easier positioning of natural clay sample edges with respect to the four corner edges of the square receiver.

6. The tests indicated that several modes of scour can occur. The ranges of tractive shear for these modes are given in table 5.

7. Values of tractive shear when general erosion was first observed ranged from 1.92 to 12.9 Pa (0.04 to 0.27 lb/ft^2). The values in table 6 can be compared with the results of the physical model shear values to help determine whether protection of clay is necessary.

8. Results of the clay sample tests indicate that all exposed clay will erode at a tractive shear of 14.4 Pa (0.3 lb/ft^2).

9. Based on distribution analyses of 1:120 model data, tractive shear of 14.4 Pa (0.3 lb/ft^2) and greater is expected to occur on 72 percent of the riverbed at a discharge of 11 335 m^3/s (400 000 ft^3/s).

10. For tractive force values determined with a model or from any other source, values from the plot on figure 18 at any selected side slope can be multiplied by tractive force to determine the gravel or rock size needed to protect the clay exposure.

RECOMMENDATIONS FOR FUTURE CLAY EROSION TESTING

1. These tests indicate that investigation of clay resistance to scour requires a multidisciplinary approach. Thus, a good program for clay erosion testing should be a combined effort including soils, hydraulics, chemical, petrographic, and geological personnel.

2. Better techniques for determining when scour starts should be investigated, and techniques for determining rates of scour should be evaluated and/or developed.

3. If the same type of equipment supplied from a high-head source is used for future testing of clay samples, control valves rather than butterfly or gate valves should be used that have more positive control characteristics and can stand long term low discharge under high head. It would be desirable to provide quick-acting clamping and effective sealing of the observation window for rapid placement and access to the samples.

4. Threshold of movement tractive shear values determined with specific test devices should be evaluated in terms of parameters developed from complete equations or sets of variables derived by dimensional analysis. Thorough analyses should also be made in an effort to quantify the degree of approximation of test devices and results in terms of all the parameters derived rather than just the one usually used in the final presentation of the data. These analyses would provide a means to determine the effects of dropping one or more of the pi (π?) terms.

LITERATURE REVIEW AND THEORY

General Considerations

Scour is a complicated interaction between riverbed soil properties, soil conditions, and bed and flow characteristics. This interaction is further complicated by the loose boundary between the flowing water and the sediment bed. Flow can change the shape of riverbeds by scour, dune movement, and deposits. A change in bed shape changes flow characteristics. Sand and gravel, when moving, can actually abrade clay exposures and, when not moving, local scour can occur around the gravel.

Soils have infinite combinations of grain size that can be expressed by statistical distributions of grain size (d) which help identify soil types. For fine-grained soils, identification is further complicated by variation in cohesiveness that can only be partially expressed by the PI (plasticity index) and the LL (liquid limit). It is desirable but difficult to express erosion resistance in terms of soil properties, state of consolidation, and geological conditions such as bedding and jointing. Calcium and sodium in the flowing water can change particle surface electrical charge that produces cohesive bonding of colloidal particles.

Fluid shear on the sediment boundary, lift, drag, secondary flows, and turbulence are considered the main factors that initiate and continue the transport of sediment. These factors are a study in themselves and vary with channel geometry and dimensionless flow parameters. (These factors should be studied separately because they vary . . . . ?)

Tractive Shear Caused by Flow

For flow in canals and rivers, the simplest expression for average tractive shear can be determined from a free body diagram for normal flow. Then

$$\tau = \frac{\gamma ALS}{PL} \qquad (1)$$

where:

τ = the tractive shear on the flow boundary

A = area of flow section

P = wetted perimeter of flow section

L = reach length in direction of flow

S = slope of bed for normal flow or energy gradient for gradually varied flow

γ = specific weight of water

By defining hydraulic radius as:

$$R = A/P \qquad (2)$$

The equation (1) can be rewritten in the more familiar form as:

$$\tau = \gamma RS \tag{3}$$

Head loss for open and closed conduit flow is frequently expressed by the generally accepted Darcy-Weisbach relationship as:

$$h_l = f \cdot \frac{L}{4R} \cdot \frac{V^2}{2g} \tag{4}$$

where symbols not previously defined are:

h_l = head loss in feet or meters of water

f = Weisbach friction factor

V = average velocity of flow

g = acceleration of gravity

Slope (S) is the same as (h_l/L) and specific weight (γ) is density (ρ) times gravity (g) or (ρg). Thus, equations (1) and (3) can be combined resulting in:

$$\tau = f\rho V^2/8 \tag{5}$$

This equation shows the relationship of tractive shear and the Darcy-Weisbach friction factor.

Tractive shear has also been related to vertical velocity profiles by logarithmic relationships by various investigators (Enger and Ellsperman, 1954). These equations can be reduced to two-point relationships. One example is the following relationship:

$$\tau = \rho \left[\frac{V_2 - V_1}{2.5 \log_e (Y2/Y1)} \right]^2 \qquad (6)$$

The two velocities (V) should be measured at relatively small distance from the bed (Y), but not so close that the pitot tube proximity to the boundary affects the velocity measurement.

A certain turbulence intensity may initiate movement. Once sediment is suspended, a somewhat less intense turbulence will keep particles in suspension. Turbulence intensity (I_t) is expressed as:

$$I_t = \frac{\sqrt{\overline{V'^2}}}{V_{a_s}} \qquad (7)$$

where (V′) is velocity fluctuation about temporal mean velocity ($\bar{V}$) at a point and (V_{as}) the mean flow section velocity. Values of (I_t) have been measured from 0.03 to 0.07. However, 0.1 is considered the value at which the velocity fluctuation can no longer be considered part of the main flow. It should be remembered that turbulence at any point is strongly affected by flow section geometry, friction factor (f), fluid properties, location with respect to boundary and form disturbance just upstream.

Velocity fluctuations are normally distributed about the mean velocity (V_μ) and therefore the largest fluctuation to be expected would be nearly (3σ) where (σ) is the standard deviation. Kalinske (1947) found that near the bed:

$$V_b \approx 4\sigma \tag{8}$$

Normal statistical distribution and equation (7) indicates that the maximum instantaneous velocity (V_b) near the bed can be 1.75 times the average velocity. Since (τ) is proportional to velocity squared (equation 4), expected maximum instantaneous shear is about three times the average shear.

Early Tractive Shear and Velocity Concepts for Incipient Transport

To attain useful scour and transport criteria, soil properties must be related to flow properties. For cohesionless soils, it is generally accepted that the weight of the largest sediment grain transported is proportionally related to velocity (V) to the sixth power of the water in the vicinity of the particle (American Society of Civil Engineers, 1975). This proportionality suggests the possibility of a transport threshold velocity (V_t) that will just move a particle of diameter (d). If particles are assumed to be spheres with constant specific weight, then weight is proportional to the diameter cubed. Combining these two proportionalities results in:

$$V_t \propto d^{1/2} \tag{9}$$

Also, equation (4) combined with equation (8) suggests the possibility of a threshold tractive shear (τ_t) or shear that will just move a particle of diameter (d) and can be written:

$$\tau_t \propto d \tag{10}$$

Although the relationships of equations (8) and (9) are frequently used with some success, they are really oversimplifications in terms of soil properties, soil conditions, and hydraulic flows.

It is generally accepted that cohesion plays an important part in scour resistance of clay soils. Sometimes the effects of cohesion are expressed by assuming that they are defined by grain size only. Sometimes more complicated approaches will assume that cohesion is a function of all or part of the following variables:

d_{50} = mean grain size

σ_d = standard deviation grain size

K_d = skewness of grain size

%C = compressive strength

S_{vs} = vane shear strength

C_s = compressive strength

PI = plasticity index

LL = liquid limit

PL = plastic limit

and others (???)

Relative Scour Resistance in Terms of Soils

Through experience, engineers develop concepts of relative resistance to erosion of soils relative to soil classification. For example, Reclamation geotechnical engineers have ranked the relative resistance to erosion of different soil types in table 1 (Gibbs, 1962). This ranking is for canals where clay embankments have been recompacted.

For soils with over 50 percent of the grain diameters less than 0.074 mm, plastic properties can contribute to erosion resistance in varying degrees from just slightly adding to the effects of grain size to being the dominant source of resistance. Plastic soil properties can be expressed at least partially by the following Atterburg limits:

Liquid limit. - LL is the water content in percent of dry weight that marks the separation between acting like a liquid or plastic.

Plastic limit. - PL is the water content at which the clay starts to act elastic rather than plastic.

Plasticity index. - PI is the difference between LL and PL and is the range of water content through which the soil has plastic characteristics.

Figure 3 taken from Gibbs (1962) shows the relative erosion resistance of cohesive soils in terms of the LL and PI. The "A-line" separates the clays from the silts below. It should be remembered that the tractive shear ranking in this chart applies to disturbed soils that were recompacted to 90 lb/ft^3. The tractive shear ranges of the laboratory data used to derive this figure are given next to the shading key.

Smeardon and Beasly (1959) did separate correlations of critical tractive shear with PI, dispersion ratio, percent clay, and mean particle size. They selected the PI and dispersion ratio as most strongly correlated. The data for these correlations were obtained in a flume with clays reformed by drain consolidation.

Carlson and Enger (1962) did multiple correlation analyses of various combinations of soil properties versus tractive shear values determined with reformed samples of clay. They found that plastic properties and densities are the most important soil properties that affect scour resistance.

Table 1, taken from Gibbs (1962), and tables 2 and 3 from Lane (1952) summarize the work of early investigators relating critical velocity and critical shear. Included in these tables are some data for cohesive soils. Etcheverry's data, table 2, for alluvial and clay soils critical tractive shear ranged from about 4.8 to 20.6 Pa (0.10 to 0.43 lb/ft^2). Fortier and Scobey's data, table 3, for alluvial silts to stiff clays, critical tractive shear ranged from about 2.4 to 12 Pa (0.05 to 0.25 lb/ft^2) for clear water and 7.2 to 22 Pa (0.15 to 0.46 lb/ft^2) for water transporting colloidal silts. The U.S.S.R. data, table 4, showed critical tractive shear values from about 1 to 30.2 Pa (0.02 to 0.63 lb/ft^2). It should be noted that these ranges include values of critical tractive shear much higher than those for recompacted samples which approach a limit of about 0.07 lb/ft^2 as given by Gibbs, Carlson and Enger, and Smeardon and Beasly. Natural undisturbed clays, in a geologic sense, are often subjected to much greater pressures for much longer periods of time than disturbed recompacted clays and this may explain some of the larger values of tractive shear.

Equations (4) and (5) do not incorporate the effects of acceleration and deceleration on average tractive shear at a flow section. These effects can be accounted for similar to Smeardon and Beasly (1959) by using the terminology in figure 4, in differential form, and equation (1) for boundary shear loss and writing the energy equation as:

$$\frac{V^2}{2g} + D + dZ = \frac{(V + dV)^2}{2g} + (D + d\,D) + \frac{\tau}{\rho g D}\,dx \qquad (11)$$

The term $(dV)^2$ is ignored because it is very small relative to $(2V\,dV)$ and solving for (τ) results in:

$$\frac{\tau}{\rho g D} = \left[- \frac{V dV}{g dx} - \frac{dD}{dx} + \frac{dZ}{dx} \right] \qquad (12)$$

This equation includes the effects of accelerating or decelerating flow. For uniform flow with small slope angles, equation (11) reduces to equation (1) because sin ϕ very nearly is equal to tan ϕ and dV and dD are zero. Thus, the term in parenthesis in equation (11) is a complex slope clearly showing some of the complications of gradually varied flow compared to uniform flow.

Dimensional Analyses

Equation (3) was used for the characteristic or tractive shear boundary value to define dimensionless tractive shear. This and the other dimensionless variables were defined:

$$\tau_* = 8\tau/f\rho V_b^2$$

$$X_* = X/X_b$$

$$D_* = D/X_b$$

$$Z_* = Z/X_b$$

Where an asterisk denotes dimensionless variables, (b) denotes boundary values and (f) is the Darcy-Weisbach friction coefficient. Solving for the dimensionless variables, substituting them into equation (11), and grouping characteristic variables with constants into terms enclosed in parentheses result in:

$$\frac{\tau_*}{D_*}\left[\frac{V_b^2}{g_b^x}\cdot\frac{f}{8}\right] = -\frac{V_* dV_*}{dX_*}\left[\frac{V_b^2 b}{g_b^x}\right] - \frac{dD_*}{dX_*} + \frac{dZ_*}{dX_*} \qquad (13)$$

where:

V_b^2/g_b^x = the Froude number squared

f/8 = a function of Reynolds number $V_b X_b/\upsilon$ and relative roughness K/4R

υ = kinematic viscosity and K is boundary surface roughness

Equation (13) is dimensionless and the terms in parentheses are equation associated dimensionless parameters or π (pi) terms. To exactly apply results from a model or from any laboratory test clay erosion test facility, all these π terms must be the same for shear test facility as well as for the river or canal in question. Satisfying this requirement would ensure that forces, turbulence, and secondary flows are similar for the actual channel and the erosion test device. In practice, complete compliance with this requirement cannot be accomplished. However, efforts should be made to determine the degree of compliance and the effects of noncompliance in the interpretation and use of data obtained with any erosion test facility.

Simons and Senturk (1977) showed by dimensional analysis that noncohesive material has an entrainment function expressed as:

$$\frac{\tau_t}{(\gamma_s - \gamma_w)d} = \phi\left[\frac{U_* k_d}{\upsilon}, \frac{d}{R_t}, \frac{\gamma_s}{\gamma_w}\right] \tag{14}$$

and shear velocity (U_*) can be defined as:

$$U_* = \sqrt{\frac{f}{8}} \cdot V = \sqrt{gR_{tS}} = \sqrt{\frac{\tau}{\rho}} \tag{15}$$

where symbols not previously defined are:

τ = subscript denoting threshold shear

s = subscript denoting sediment

w = subscript denoting water

Using the π term (d/Rt) and valid pi term manipulation, (d) can optionally be replaced by (R) in any of the other π terms resulting in an equally valid relationship. Thus,

$$\frac{\tau_t}{(\gamma_s - \gamma_w)R_t} = \phi\left[\frac{U_{*_t} R_t}{\nu}, \frac{d}{R_t}, , \frac{\gamma_s}{\gamma_w}\right] \tag{16}$$

The π term on the left can be considered the dimensionless shear or shear velocity grain Froude number and the first π term in the parentheses is the shear velocity grain Reynolds number.

Substituting the first form of equation (14) and (15) results in:

$$\frac{\tau_t}{(\gamma_s - \gamma_w)R_t} = \phi\left[\frac{V_c R_c}{\nu}\sqrt{\frac{f}{8}}, \frac{d}{R_t}, \frac{\gamma_s}{\gamma_w}\right] \tag{17}$$

If cohesive erosion resistance (E_r) could be defined in some dimensionless form in terms of cohesive soil properties, it could be added to equation (16). For relatively deep flow or relatively fine sediment and for water and constant (γ_s), the last two π terms can be dropped from entrainment functions and

$$\frac{\tau_t}{\left(\frac{\gamma}{s} - \gamma_w\right)R_t} = \phi\left[\frac{V_t R^4 t}{\nu}, \frac{f_t}{8}, E_r\right] \tag{18}$$

Using equation (3) to replace (V) and squaring, results in an alternate dimensionless equation that is more readily defined by hydraulic measurements expressed as:

$$\frac{\tau_t}{(\gamma_s - \gamma_w)R_t} = \phi\left[\frac{S_t R^3 t\, g}{\upsilon^2}, E_r\right] \tag{19}$$

These equations show that threshold of sediment movement shear (τ_t) determined from a test device should be used for design with care. Some sort of adjustment should be made to account for lack of complete hydraulic similitude between erosion test devices and the actual channels. Thus, equation (17a) and (17b) could be used to help evaluate an erosion test facility and to help account for scale effects between test

facilities and the actual flow channels. However, (R) is constant for the duct used in this study and could not be varied to determine the functional relationship without further test results from other duct or open channel shapes and sizes.

These equations cannot account for bedding planes and geological conditions of the soil such as clay jointing. The soil properties that control flaking or pitting erosion between adjacent layers of clay would be difficult to ascertain, if at all possible. Thus, equations (17a) and (17b) apply to homogeneous parts of clay samples only. The problems of applying threshold tractive shear values from a test device to river channels with different friction and hydraulic radius values applies to both massive and bedded clay.

In empirically defining relationships (17a) and (17b), it would be best to use measured values of standard clay soil properties determined by laboratory tests. If possible, a single clay soil property, such as cohesion or unconfined shear strength, should be related by dimensional analysis to other soil properties that affect erosion resistance rather than combining hydraulic and soil properties. Other possible soil properties that could be incorporated in this analysis are PI, LL, compaction, voids ratio, Na, Ca, and dispersion. When a possible clay soil property parameter (E_r) is found, it should be tried in equations (17a) and (17b) as nesting surface parameter.

For homogeneous clays, most investigators (March et al., 1967) visually determine when threshold sediment transport tractive shear has been exceeded. Some use erosion indexes or intercepts from dimensionless plots including time and depth of erosion. Other investigators used weight loss indexes from weight versus time plots. Turbidity change of flowing water with time has also been used. Most of these methods could not be used because of the size and condition of naturally bedded, jointed samples, and the various modes of erosion. Therefore, visual observations were used for the Columbia River bottom clay samples.

THE EROSION TEST FACILITY

General Considerations

Because of reported large platelet 102- by 38- by 6-mm- (4- by 1-1/2- by 1/4-in) type erosion, large samples were necessary. It was decided that a 0.3-m-square (1-ft-square) sample surface exposed to flow was the minimum useful size sample that could be used. Divers had difficulty bringing up cubic foot particle samples. Thus, it was decided to use 0.3- by 0.3- by 0.15-mm (12- by 12- by 6-in) samples. The only way to provide uniform tractive shear over a clay sample of this size is to take advantage of the wide lateral distribution of uniform velocity in the middle part of a wide rectangular duct. It was decided to use a 0.91- by 0.10-m (36- by 4-in) duct to produce tractive shears as high as those determined with the 1:120 physical model. The shallow duct with Plexiglas viewing window (fig. 5) in the top of the duct would also provide a close equidistant view over the sample without water surface disturbances interfering with viewing. A photograph of the test facility is shown on figure 6.

Instrumentation

Flow through the clay erosion test duct was measured with a venturi meter in the 0.41-m- (16-in-) diameter approach pipe. A mercury pot gauge and blowdown water piezometers were used to measure high and low venturi pressure differentials, respectively.

Velocity profiles were measured with a Prandtl tube. The dynamic and static heads were measured by pressure cells. Zero and full scale output were set and checked using the micromanometer shown on figure 7.

Calibration Tests

Vertical velocity profiles over the middle of a dummy sample were obtained for several discharges ranging from 0.3 to 3.81 m/s (1 to 12.5 ft/s). Examples of these profiles are shown on figure 8 plotted in semilog form. These velocity profiles show that the logarithmic velocity distribution assumption was valid at least down to 10 mm (0.033 ft) from the bed. Tractive shear was determined from the velocity profile measurements and using equation (5). While velocity profiles were being measured, the differential of the venturi meter was read. A plot of venturi differential pressure versus computed tractive shear in the duct was used during the sample testing for quick estimation of tractive shear across each sample.

Sampling Technique

The Pacific Northwest Region diving team developed the clay sampling technique. Divers cut the sample out with a pneumatic underwater power saw. Plastic boxes with beveled edges were slipped over the samples for handling. Figure 9 shows two dried-up practice samples in plastic boxes; note the layered characteristics. Four samples in submerged storage in watering tank are shown on figure 10. These samples were submerged and stored from 2-1/2 up to 4 weeks in the plastic handling boxes. Fat clay samples stored better than silty or lean clays whose outer surfaces became mushy. Some samples stuck to the bottom of the sample handling boxes. Figure 11 shows the top layer of a sample that stuck to the bottom of the handling box. It was found that gently blowing air into the vent holes in the box bottom while lifting the plastic box helped prevent sticking.

Only one natural riverflow surface layer of the samples was suitable for shear testing. Handling damage and/or natural jointing precluded the possibility of adequate support of the natural riverflow surface in the

sample receiver during shear testing. There was one case of a top layer drying and bending relative to the more moist adjacent layer underneath the parting layer.

A piece of flow-sculptured surface that was removed to obtain a surface intact enough for support in the receiver is shown on figure 12. The dimpling is commonly seen in early sculpturing of fat clay. The figure also shows the bottom of the piece with leaner sandy clay lamina adjacent to a fatter clay lamina.

Figure 13 shows an open jointed piece of flow surface with more fully developed sculpturing where dimples have elongated and come together. The figure also shows the inside of the parted open joint where parts of clay lamina and a silty clay lamina adhered to each other. One side shows a spherical depression and the other side shows its companion spherical mound. This is thought to be a cast resulting from a piece of gravel deposited from floating, gradually melting glacial ice. The gravel partially settles into the loose clay layer already on the bottom then is covered by slower settling fines. Figure 14 shows a kidney shaped scour hole caused a piece of gravel released from a cast by previous scour.

It is generally accepted that as flow surface sculpturing progresses from light dimpling to deeper scour elongation, sediment transport increases. Some initial dimpling action was observed in the test duct on a fat clay layer. Shallow, and barely discernible dimples gradually appeared without any observable cloudy transport because of being washed away by the flow.

Test Procedure

The samples were carefully taken from the submerged storage tank and turned over with a plywood board on top. Project soils laboratory personnel removed the plastic sample box and carefully trimmed the sample to fit the sample receiver. The samples were lowered to be as flush as possible with the bottom

flow surface of the duct. After securing the plastic viewing window, the duct and tailbox were gradually filled with plant service water until the duct exit was fully submerged. Then the valve controlling the test duct waterflow from the cooling water system was opened slightly. Clay samples were watched continually for at least 15 minutes, and venturi head differentials were recorded. The process of increasing the flow slightly, observing samples, and reading the differential was repeated until sufficient observation of general erosion was made and/or the exposed sample lamina was damaged beyond further use for testing or needed to be reset flush to the duct bottom. If enough sample remained and was not too loosely jointed to provide proper support of the sample in the receiver, it was raised and cut to a new flow surface for repeated testing.

RESULTS

Modes of Erosion

The following modes of erosion were noted during the testing of the river bottom clay samples:

Particle emergence. - Scattered sand and gravel emerged from layers of silt or clay due to local scour around the particles.

Pitting. - Scattered pits formed in and through thin layers of silt or clay due to local spots or weakness, such as sparsely scattered clusters or casts of particles on or in layers of more cohesive clay.

Lining. - Multiple parallel lines gradually appeared on areas of the samples possibly due to paper-thin bedding with slight dip.

Incising. - Any slight scratch on the sample flow surface, in any direction with respect to the flow, grew deeper. Perpendicular lines often formed on the slopes leading out of the incised scratches. The initial scratches could have been caused by sliding or rolling gravel, by waterlogged twigs or branches moving in contact with the river bottom, and by animal contact.

Venting. - When joints are open, water can flow through them. If the internal joint flow velocity is sufficient, relative to the particle bonding,then colloidal plumes come out in spots and lines along the open sample joints at the flow-bed interface.

Flaking. - Flaking was caused by bedding weaknesses existing prior to testing and removed by the flow or by further weakening by water entering into porous layers or into open joints. Sizes of flakes ranged from small paper-thin bits up to platelets about 102 by 38 by 6 mm (4 by 1-1/2 by 1/4 in) thick previously reported by divers.

Rocking. - In loosely jointed samples with interlocking networks of fractures, certain pieces would rock and vibrate but not leave the sample. Thus, there was a grinding action between pieces within the joints. There was also a chipping action along the edges of the joints at the interface between the flow and the bed.

Chunking. - Transport pieces larger than platelet size were arbitrarily called chunks. These chunks ranged from about 76 by 76 m (3 by 3 in) up to 152 by 305 mm (6 by 12 in). The larger size was, of course, limited by the clay sample size. Chunks up to 1 inch thick were noted.

Dimpling. - Light spherical depressions were occasionally observed on flat flow surfaces of fat clay samples. The process was very slow and no cloudy clay transport was visible. It was as if invisible fingers were gently pressing and forming the dimples.

Observed tractive shear and the average duct velocity ranges related to these different modes of erosion are given in table 5. During observation of the 7 clay samples, 15 runs of measured tractive shear values ranged from 0.24 to 182 Pa (0.005 to 3.8 lb/ft^2).

Tractive Shear Causing Erosion of Samples

Tractive shear causing first general erosion determined for the clay samples are given in table 6 along with corresponding average duct velocities and modes of erosion. Tractive shear when erosion was first observed ranged from 1.9 to 12.9 Pa (0.04 to 0.27 lb/ft^2) with corresponding average duct velocity ranging from 0.52 to 1.34 m/s (1.7 to 4.4 ft/s). Considering the 15 clay surfaces tested as random samples, the cumulative distribution of tractive shear values for initial observed erosion is plotted on figure 15. Based on this plot, it is estimated that 3 percent of the river clay area would erode if exposed to a tractive shear of about 0.96 Pa (0.22 lb/in^2), 50 percent at 4.8 Pa (0.1 lb/ft^2)m and 95 percent at 10.5 Pa (0.22 lb/ft^2). All the samples eroded at less than 14.4 Pa (0.30 lb/ft^2).

Tractive Shear Caused by Riverflow

Field values of tractive shear for riverflow of about 2380 m^3/s (84 000 ft^3/s) and 1:120 model values for flows of 4530, 6800, and 11 300 m^3/s (160 000, 240 000, and 400 000 ft^3/s) were used to estimate cumulative distribution of shear on the entire riverbed studied with the 1:120 scale physical model. The number of tractive shear values determined from vertical velocity profiles at each of the discharges were

19, 36, 45, and 46, respectively. The resulting cumulative distributions are plotted on figure 16. These curves can be used to estimate the percent of the riverbed that would be exposed to a given tractive shear value or less.

Based on diver reports, it is estimated that 1 percent of riverbed modeled from the dam to STA 3109 (Sta. 102+00) is exposed clay. It was previously stated that all of the riverbed clay was expected to erode at a tractive shear of 14.4 Pa (0.30 lb/ft^2) or less. From figure 16, it is estimated that at discharges of 11 300, 6800, 4530, and 2380 m^3/s (400 000, 240 000, 160 000, and 84 000 ft^3/s) tractive shear of 14.4 Pa (0.30 lb/ft^2) is equaled or exceeded on about 72, 63, 45, and 40 percent of the riverbed. The unusual way the discharge curves nested could be the result of change of river shape, overbanking, or sample defect, such as small number or lack of randomness.

Protective Gravel Blanket Design

Gessler (1968) modified Shields' entrainment function by adding probability of moving out of a mixture of sediment sizes as a third parameter. The Gessler function is shown on figure 17. The ordinate and abscissa are the same parameters as the first two given in equation (13). For grain Reynolds numbers greater than 400, dimensionless shear becomes constant at a designated C_p value. Thus, for any selected probability, p, of moving,

$$\tau_p = (\gamma_s - \gamma_w)dC_p = K_p d \qquad (20)$$

where τ_p is shear causing movement at probability p, d is diameter of a sediment particle, γ_s, is specific weight, and s and w are subscripts denoting sediment and water. For probabilities of 0.05, 0.5, and 0.85, C_p values are about 0.024, 0.047, and 0.12, respectively.

An approach similar to Carlson (1966) for correcting for slope gravity effects was combined with Gessler's entrainment function. The main hypothesis was that the resistance to motion, on the transverse side slope and on the level bottom, is equal to the normal force times the tangent of the angle of repose for the bed material. Taking the ratio of the force on the slope to the force on the level and assuming spherical particles results in:

$$\tau_s/\tau_l = \cos\phi \ (1 - \tan^2\phi/\tan^2\theta)_{1/2} (d_s/d_l) \qquad (21)$$

where τ is tractive shear, Φ is the angle of the side slope, Θ is the angle of repose, d is the particle diameter, (s) is a subscript denoting side slope, and (l) is a subscript denoting on a level surface. Taking this equation, using equation (18) to substitute for τ_l, calling the trigonometric function the gravity correction factor K_g, and solving for d_s, result in:

$$d_s = \tau_s/K_p K_g \qquad (22)$$

Values of $(1/K_pK_g)$ are given on figure 18 for an angle of repose of 42° and specific gravity of 2.65. Figure 18 should not be used for particle diameters of less than about 10 mm (3/8 in) because of limitation in equation (18) caused by small grain Reynolds numbers.

For tractive force values determined with the model or from any other source, the plot in figure 18 can be used to determine the combined coefficient($1/K_pK_g$) that includes Gessler's probability of moving and the effect of gravity due to embankment slopes. Multiplying the tractive force by the coefficient results in the particle size. Using a probability of 0.85 gives the size that would be in general bed movement, using probability of 0.5 would result in the size nearest to that which would be obtained from critical tractive shear. Using a probability of 0.05 recommended for gravel blanket protection design would give the sizes which would rarely move on the bed. Figure 18 indicates that erosion stability decreases rapidly as side slopes get greater than 2:1. In fact, $1/K_pK_g$ asymptotically approaches infinity at the angle of repose of 42° or Z of 1.11 because K_g in equation (20) approaches zero. Thus, it is recommended that 2:1 slopes be considered the maximum allowable. Figure 18 also shows that for practical purposes, slopes of 5:1 and greater can be considered flat in terms of gravel blanket stability; values of $1/K_pK_g$ are within 5 percent of flat bed values at this side slope.

Determination of exact critical tractive shear values could not be made nor could the rate of erosion be predicted with the shear test duct. However, the observation of clay erosion modes and the distribution curves on figures 15 and 16 provide more insight and erosion prediction capability than existed before the tests. As previously stated, the diving team recorded 0.015 to 0.15 m (0.05 to 0.5 ft) erosion in 1 to 3 years of observation.

The gravel blanket design curve on figure 18 and equation (20) can be used to determine the rock diameter that will protect exposed clay on a rive bottom when the tractive shear is known. Care should be exercised in placing gravel blankets through fast flowing water to provide complete cover of exposed clay. A blanket edge in any direction, on clay, can cause local scour along the edge. Sparsely distributed cobbles on clay can cause local scour around and downstream of the individual cobbles. It is suggested that diver inspections be made of blanket placements.

BIBLIOGRAPHY

American Society of Civil Engineers, Manuals and Reports on Engineering Practice No. 54, Sedimentation Engineering, Vanoni, Vito A., editor, p. 93, 1975.

Carlson, E. J., *Critical Tractive Forces on Channel Side Slopes in Coarse Noncohesive Material*, Report No. Hyd-366, Bureau of Reclamation, 1966.

Carlson, E. J., and P. F. Enger, *Studies of Tractive Forces of Cohesive Soils in Earth Canals*, Report No. Hyd-504, Bureau of Reclamation, 1962.

Enger, P. F., L. M. Ellsperman, *Hydraulic and Bituminous Studies of Ainsworth Canal Dune Sand*, Report No. Hyd-393, Bureau of Reclamation, 1954.

Gessler, Johannes, *The Beginning of Bedload Movement of Mixture Investigated as Natural Armoring in Channels*, Translation T-5, Keck Laboratory, California Institute of Technology, October 1968.

Gibbs, H. J., *A Study of Erosion and Tractive Force Characteristics in Relation to Soil Mechanics Properties*, Report No. EM-643, Bureau of Reclamation, 1962.

Kalinske, A. A., "Movement of Sediment as Bed-Load in Rivers," Transactions, American Geophysical Union, vol. 28, No. 4, 1947.

Lane, E. W., *Progress Report on the Design of Stable Channels*, Bureau of Reclamation Report No. Hyd-352, 1952.

March, F. D., E. T. Smeardon, and P. F. Enger, "Erosion of Cohesive Sediments," ASCE Task Committee Report, 1967.

Simons, D. B., and F. Senturk, "Sediment Transport Technology," Water Resources Publications, Fort Collins, CO, 1977.

Smeardon, E. T., and R. P. Beasley, "The Tractive Force Theory Applied to Stability of Open Channels in Cohesive Soils," Research Bulletin 715, University of Missouri, 1959.

Table 1. - Soil classification with relative erosion stability.

Major divisions of soils	Typical names of soil groups	Group symbols	Erosion resistance*
FINE-GRAINED SOILS[1]	Inorganic silt, micaceous or diatomaceous fine sandy of silty soils, elastic silts	MH	
Silts and clays LL less than 50	Inorganic clays of high plasticity, fat clays	CH	12
	Organic clays of medium to high plasticity	OH	
Silts and clays LL less than 50	Inorganic and very fine sands, rock flour, silty or clayey fine sands with slight plasticity	ML	
	Inorganic clays of low to medium plasticity, gravelly clays, sandy clays, silty clays, lean clays	CL	11
	Organic silts and organic silt-clays of low plasticity	OL	
COARSE-GRAINED SOILS[2]			
Sands[3]	Silty sands, poorly graded sand-silt mixtures	SM	10 coarse
Sands with fines (appreciable amount of fines)	Clayey sands, poorly graded sand-clay mixtures	SC	7
	Sand with clay binder	SW-SC	6
Clean sands (little or no fines)	Well-graded sands, gravelly sands, little or no fines	SW	8
	Poorly graded sands, gravelly sands, little or no fines	SP	9 coarse
Gravels[4]		GW	5
Gravels with fines (appreciable amount of fines)	Silt gravels, poorly graded gravel-sand-silt mixtures	GP	3
	Gravel with sand-clay binder	GW-GC	-
Clean gravels (little or no fines)	Well-graded gravels, gravel-sand mixtures, little or no fines	GW	2
	Poorly graded gravels, gravel-sand mixtures, little or no fines	GP	3
Highly organic soils	Peat and other highly organic soils	PT	-

[1] More than half of material is smaller than No. 200 sieve size. (The No. 200 sieve size is about the smallest particle visible to the naked eye.)
[2] More than half of material is larger than No. 200 sieve size. (For visual classifications, the 1/4-in size may be used as equivalent to the No. 4 sieve size.)
[3] More than half of coarse fraction is smaller than No. 4 sieve size. (For visual classifications, the 1/4-inch size may be used as equivalent to the No. 4 sieve size.)
[4] More than half of coarse fraction is larger than No. 4 sieve size.
* Numbers indicate the order of increasing values for the physical property name.
Numbers indicate relative suitability (1 = best).

Table 2. - Comparison of Etcheverry's maximum allowable velocities with tractive forces values.

Material	Value of Manning's n used	Velocity (ft/s)	Tractive force (lb/ft^2)
Very light pure sand of quicksand character	0.020	0.75-1.00	0.006-0.011
Very light loose sand	0.020	1.00-1.50	0.011-0.025
Coarse sand or light sandy soil	0.020	1.50-2.00	0.025-0.045
Average sandy soil	0.020	2.00-2.50	0.045-0.084
Sandy loam	0.020	2.50-2.75	0.070-0.084
Average loam, alluvial soil, volcanic ash soil	0.020	2.75-3.00	0.084-0.100
Firm loam, clay loam	0.020	3.00-3.75	0.100-0.157
Still clay soil, ordinary gravel soil	0.025	4.00-5.00	0.278-0.434
Coarse gravel, cobbles and shingles	0.030	5.00-6.00	0.627-0.903
Conglomerate, cemented gravel, soft slate, tough hardpan, soft sedimentary rock	0.025	6.00-8.00	0.627-1.114

1 ft/s = 0.3048 m/s.
1 lb/ft^2 = 47.88 Pa.

Table 3. - Comparison of Fortier and Scobey's limiting velocities with tractive force values.

Material	n	For clear water		Water transporting colloidal silts	
		Velocity (ft/s)	Tractive force (lb/ft^2)	Velocity (ft/s)	Tractive force (lb/ft^2
Fine sand colloidal	0.020	1.50	0.027	2.50	0.075
Sand loam noncolloidal	0.020	1.75	0.037	2.50	0.075
Silt loam noncolloidal	0.020	2.00	0.048	3.00	0.11
Alluvial silts noncolliodal	0.020	2.00	0.048	3.50	0.15
Ordinary firm loam	0.020	2.50	0.075	3.50	0.15
Volcanic ash	0.020	2.50	0.075	3.50	0.15
Stiff clay very colloidal	0.025	3.75	0.26	5.00	0.46
Alluvial silts colloidal	0.025	3.75	0.26	5.00	0.46
Shales and hardpans	0.025	6.00	0.67	6.00	0.67
Fine gravel	0.020	2.50	0.075	5.00	0.32
Graded loam to cobbles when noncolloidal	0.030	3.75	0.38	5.00	0.66
Graded silts to cobbles when colloidal	0.030	4.00	0.43	5.50	0.80
Coarse gravel noncolloidal	0.025	4.00	0.30	6.00	0.67
Cobbles and shingles	0.035	5.00	0.91	5.50	1.10

1 ft/s = 0.3048 m/s.
1 lb/ft^2 = 47.88 Pa.

Table 4. - U.S.S.R. limiting velocities and tractive forces in cohesive material.

Descriptive term	Compactness of bed							
	Loose		Fairly compact		Very compact		Compact	
Voids ratio	2.0-1.2		1.2-0.6		0.6-0.3		0.3-0.2	
Principal cohesive Material of bed	Limiting mean velocity ft/s and limiting tractive force lb/ft^2							
	ft/s	lb/ft^2	ft/s	lb/ft^2	ft/s	lb/ft^2	ft/s	lb/ft^2
Sandy clays (sand content less than 50 percent)	1.48	0.040	2.95	0.157	4.26	0.327	5.90	0.630
Heavy clayey soils	1.31	0.031	2.79	0.141	4.10	0.305	5.58	0.563
Clays	1.15	0.024	2.62	0.124	3.94	0.281	5.41	0.530
Lean clayey soils	1.05	0.020	2.30	0.096	3.44	0.214	4.43	0.354

1 ft/s = 0.3048 m/s.
1 lb/ft^2 = 47.88 Pa.

Table 5. - Modes of erosion and tractive shear and velocity ranges.

Mode of erosion	Tractive shear lb/ft^2	Velocity ft/s
Scattered sand and gravel emergence from out of layers of silt and clay	0.01 to 0.015*	0.88 to 1.05*
Scattered pitting through thin silt and clay layers	0.03 to 0.12	1.50 to 2.95
Multiple or general lining and scratch incising	0.04 to 0.30	1.73 to 4.60
Venting with flow through open joints and colloid pluming	0.14 to 0.20	3.18 to 3.78
Small pieces, paper-thin flakes	0.04 to 0.20	1.73 to 3.78
Dime- to quarter-size flakes 1.8 to 1/4 inch thick	0.06 to 0.50	2.10 to 5.90
Larger flakes half-dollar size to larger 1/4 inch thick	0.06 to 0.90	2.10 to 7.80
Rocking of interlocking joint pieces	0.14**	3.18**
Chunks 3 by 3 inches and larger up to 1 inch thick	0.15 and 3.8	3.30 to 16.0

* Values are less than any tractive shear noted for general erosion because sand and gravel were so sparsely distributed.
** Only one case noted.

1 ft/s = 0.3048 m/s.
1 lb/ft^2 = 47.88 Pa.

Table 6. - Threshold tractive shear and velocity when general erosion was first observed.

Sample No.	Run No.	Threshold tentative shear (lb/in^2)	Average duct velocity (ft/s)	Mode of erosion noted
1	1	0.16	4.3	Flaking
	2	0.12	2.9	Flaking
	3	0.09	2.6	Pitting and incising
2	1	0.04	1.7	Pitting and flaking
	2	0.04	1.7	Pitting and flaking
	3	0.10	2.7	Slow pitting
3	1	0.08	2.4	Chunking
	2	0.20	3.8	Flaking
	3	0.19	3.7	Flaking and venting
4	1	0.27	4.4	Incising and lining
	2	0.18	3.7	Incising
5	1	0.17	3.5	Pitting and flaking
	2	0.11	2.8	Flaking
6	-	Not tested	-	Sample totally damaged
7	1	0.06	2.1	Flaking
8	1	0.08	2.4	Flaking

1 ft/s = 0.3048 m/s.
1 lb/ft^2 = 47.88 Pa.

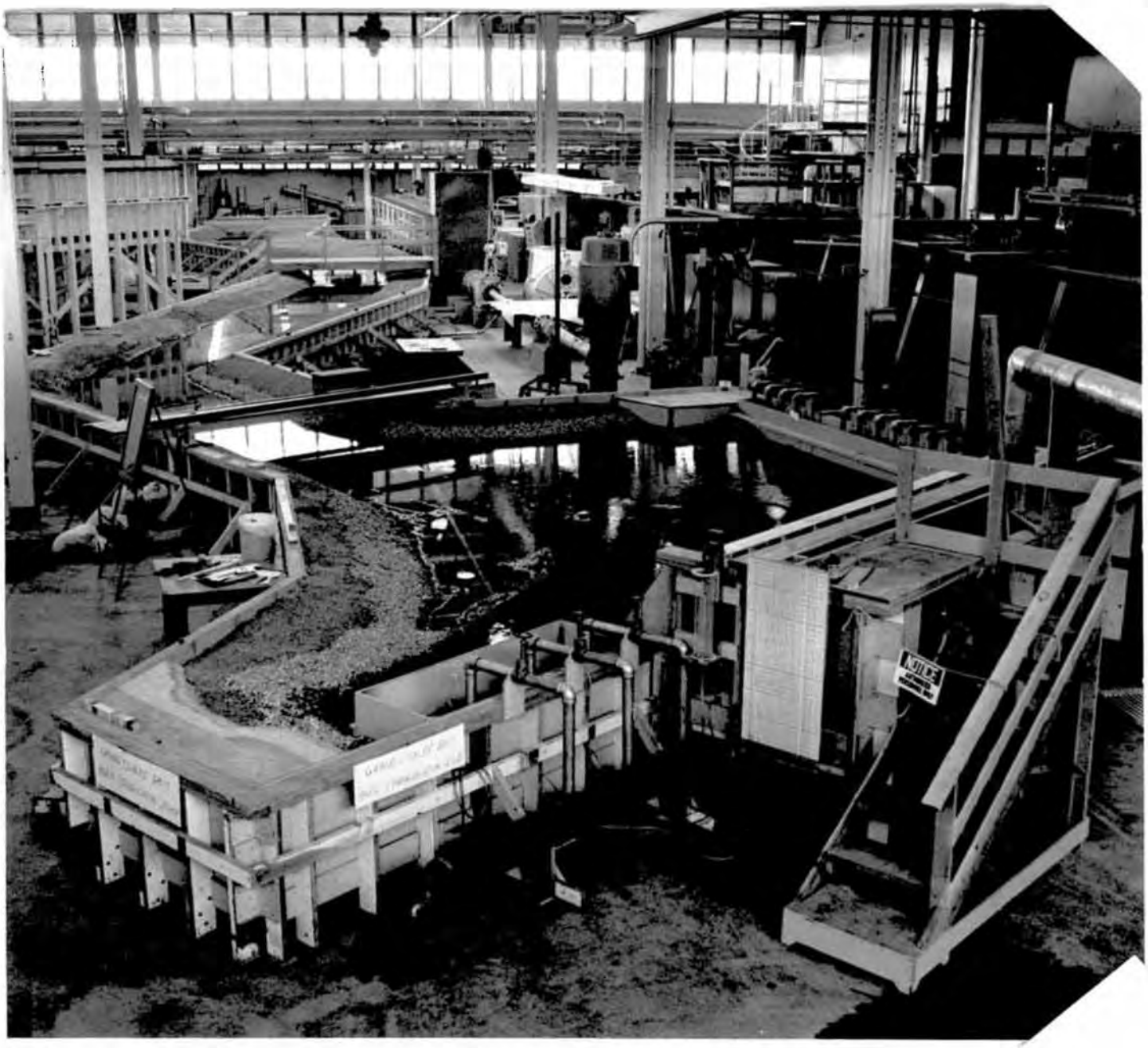

Figure 1. - The 1:120 scale physical model used to determine tractive shear on riverbed.

Figure 2. - Platelet type of erosion from bedded clay transported 366 mm (1200 ft). Project photograph by T. J. Spicher.

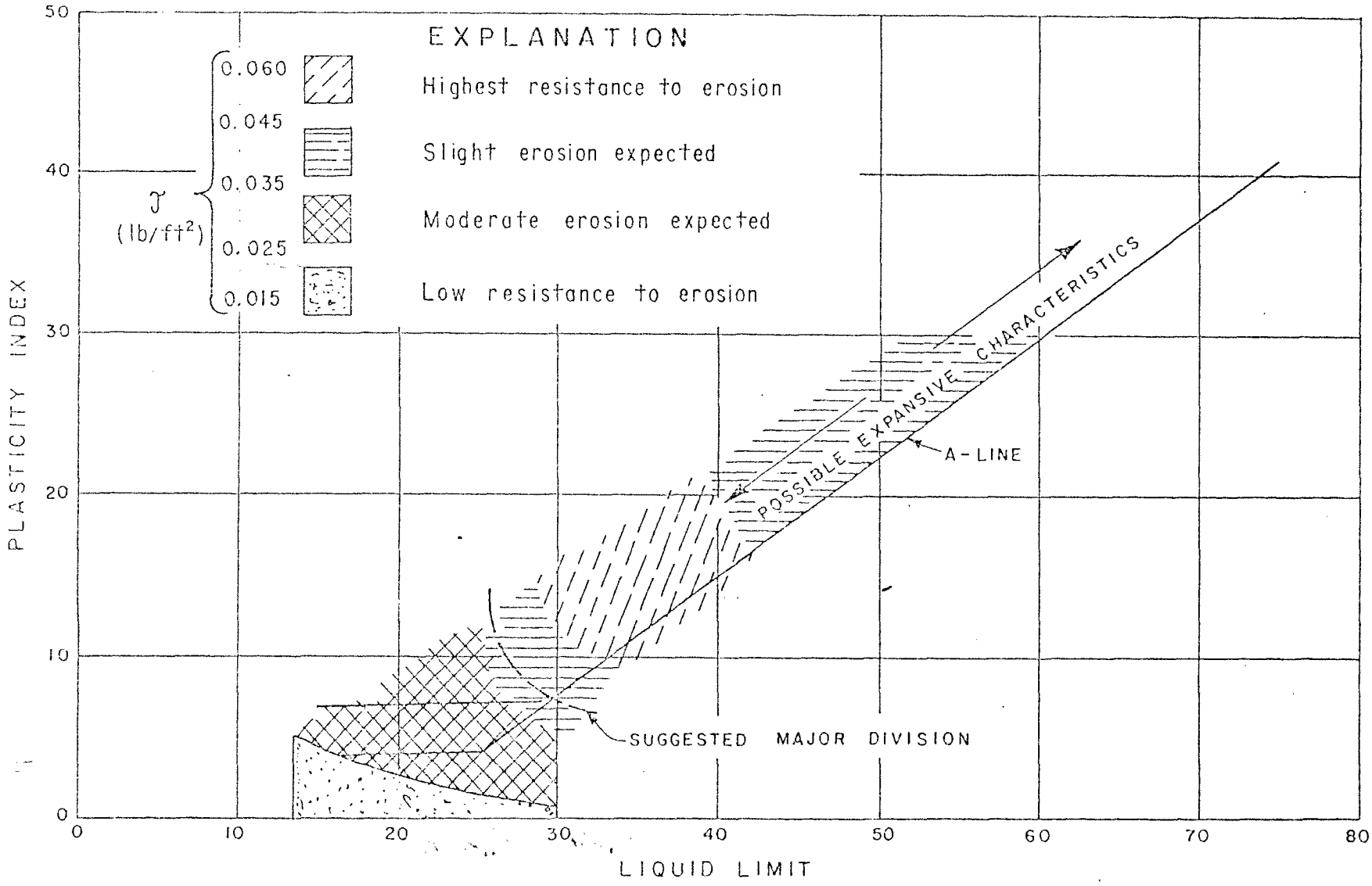

Figure 3. - Erosion characteristics for fine grain soils with respect to plasticity index. Taken from Gibbs (1962).

$$V = q / D$$

$$\frac{dv}{dx} = \frac{-q}{D^2} \frac{dD}{dx}$$

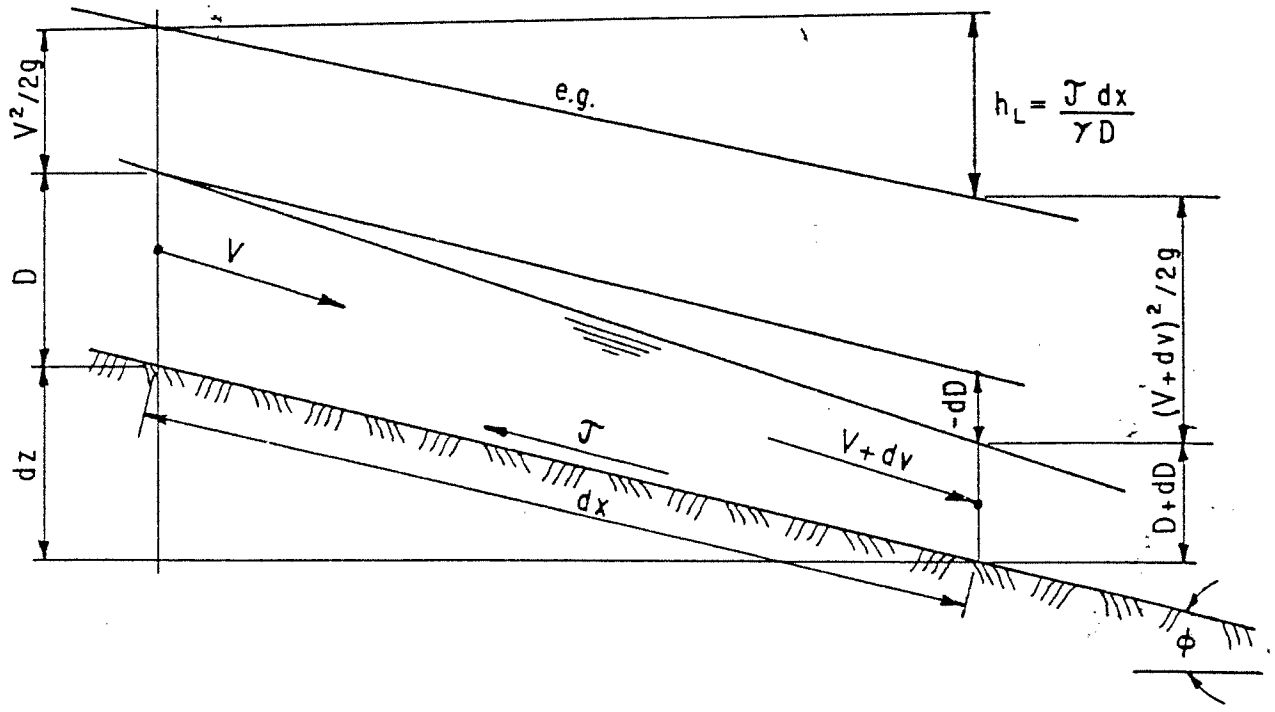

Figure 4. - Definition sketch for gradually varying flow.

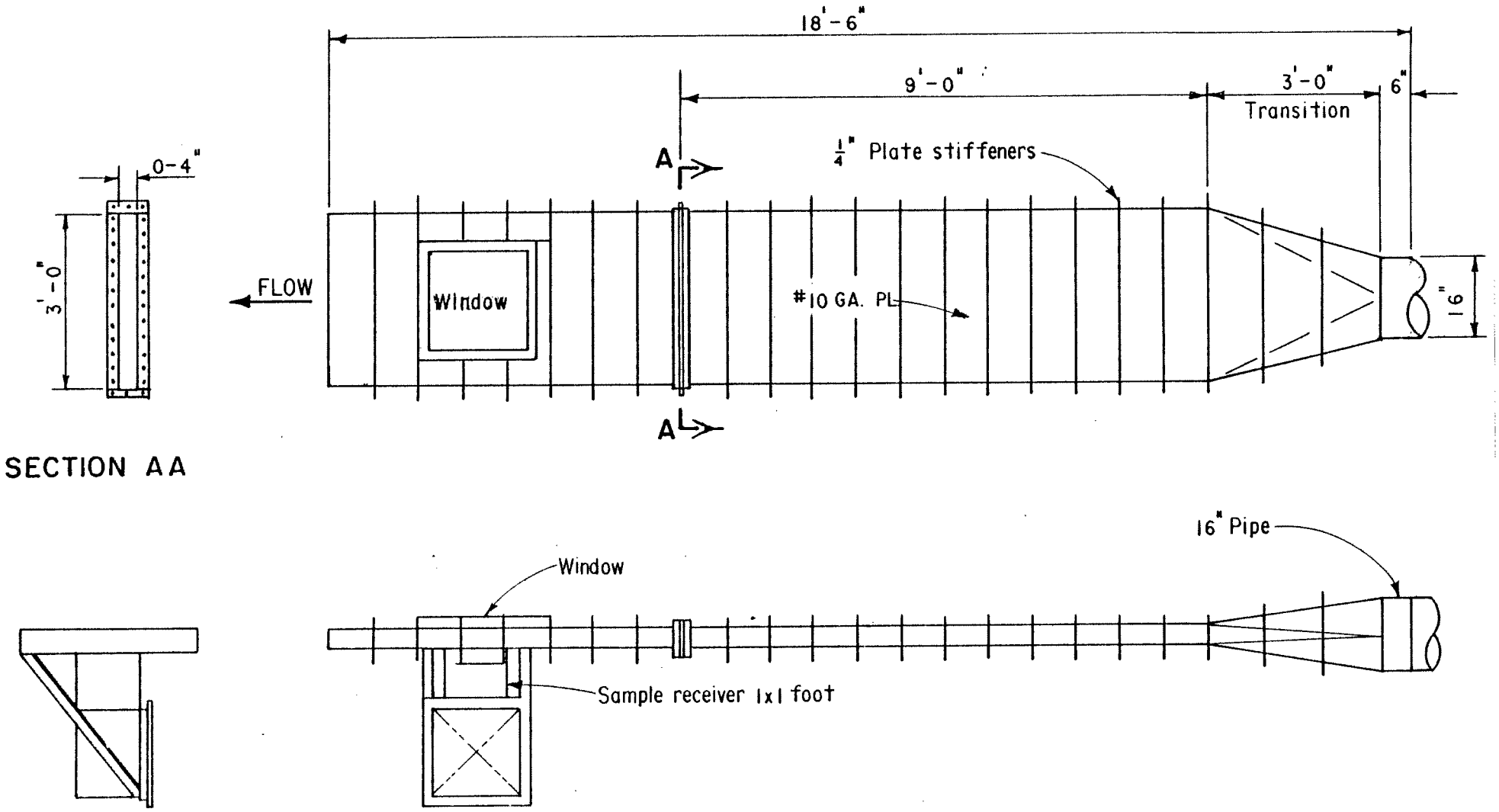

Figure 5. - Shop drawing of tractive shear test duct.

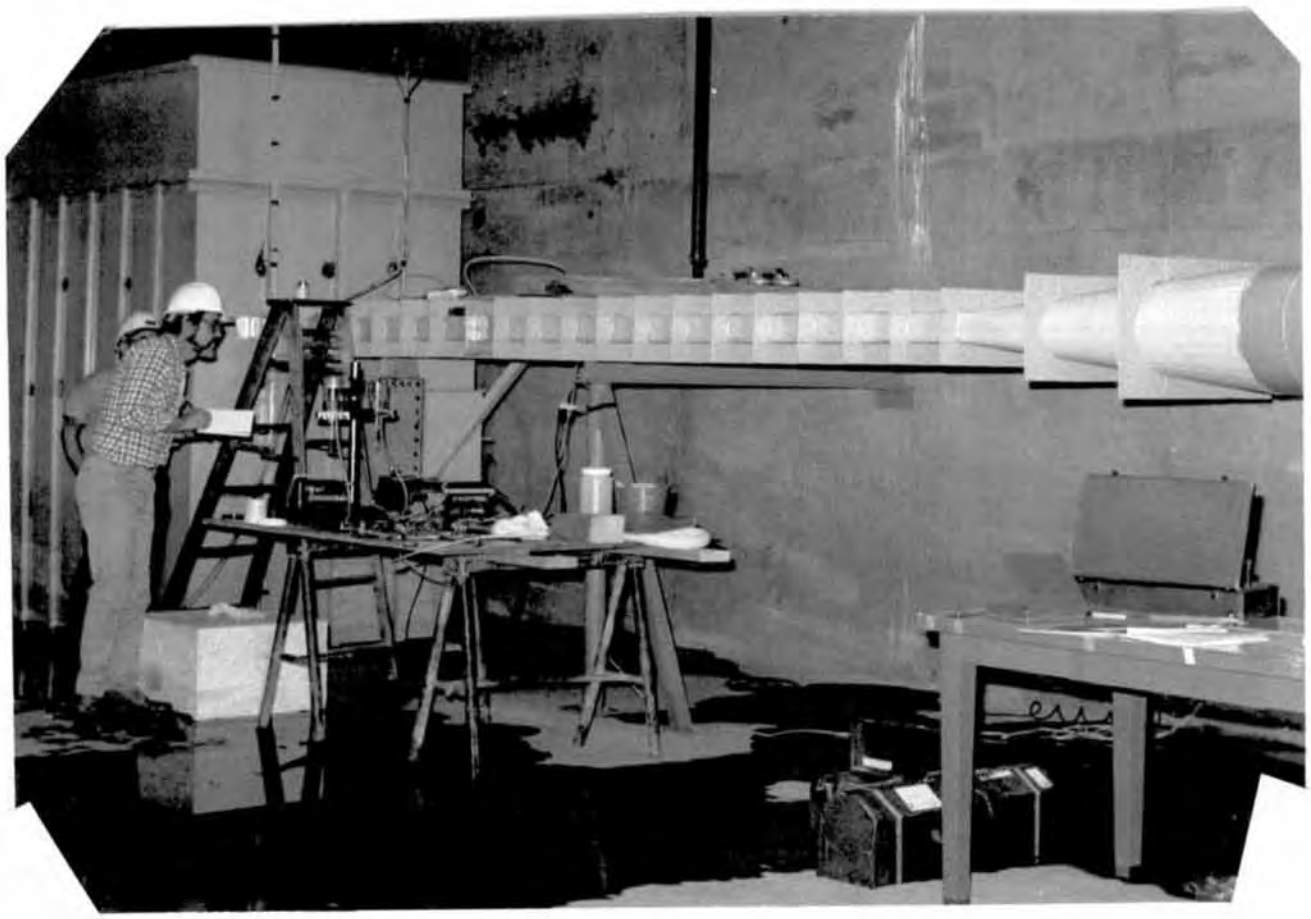

Figure 6. - Tractive shear test duct in the Third Coulee Powerplant. GCPO photograph.

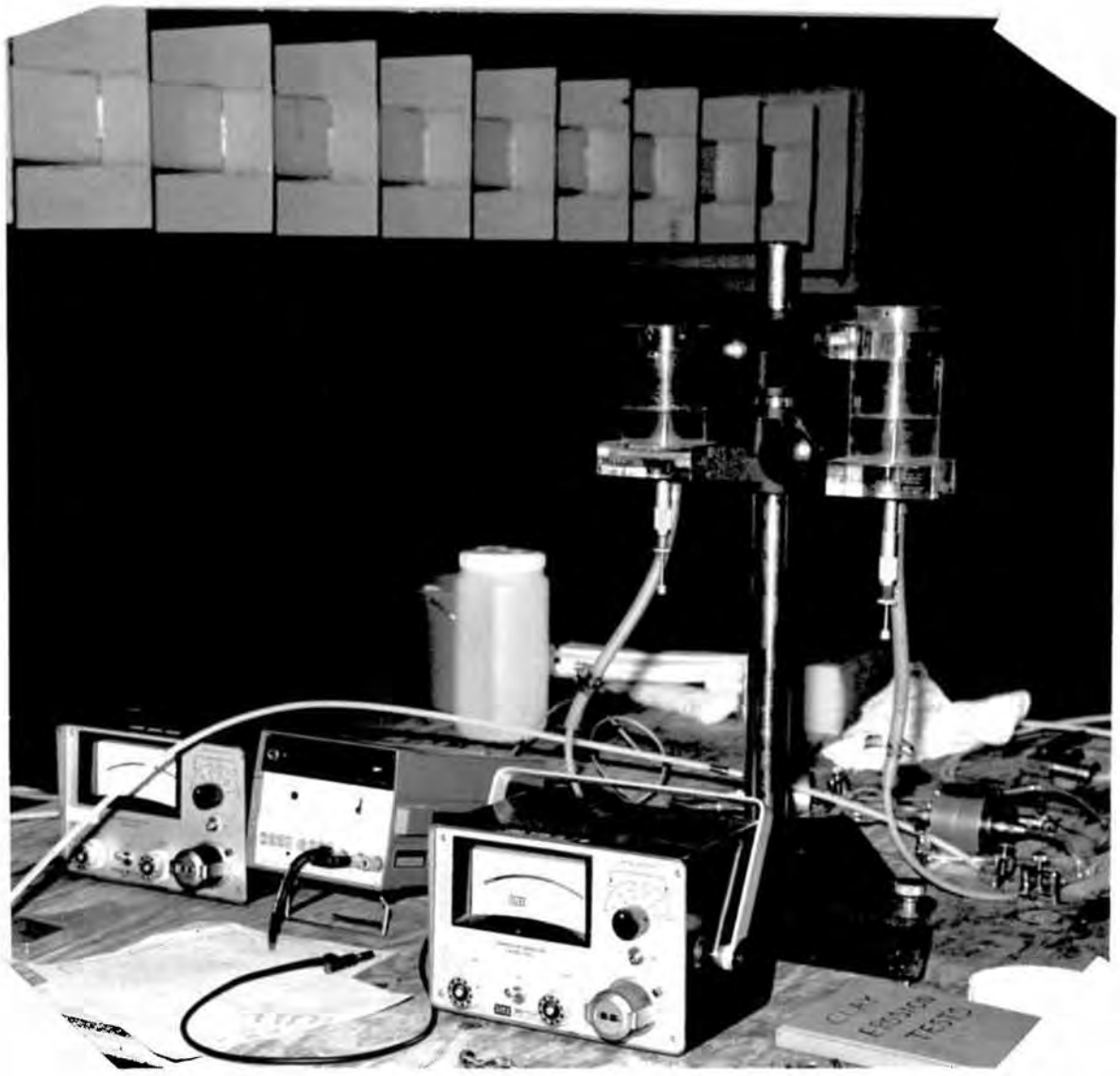

Figure 7. - Micromanometer used to calibrate pressure cells for pitot velocity measurements.

Figure 8. - Velocity profiles over center of sample area for various discharges.

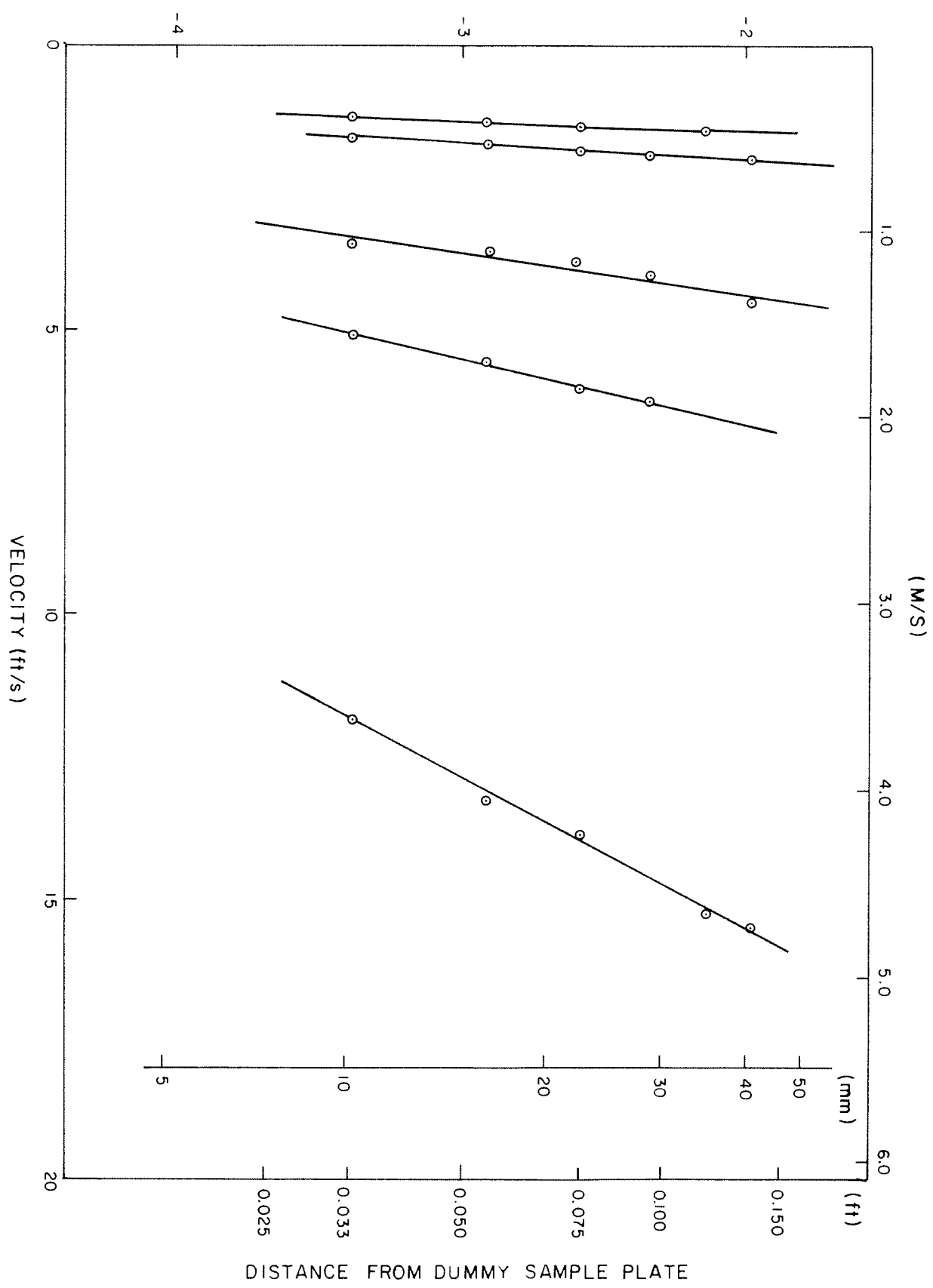
LOGe OF DISTANCE FROM DUMMY SAMPLE PLATE
-4
-3
-2
0
5
10
15
20
VELOCITY (ft/s)
1.0
2.0
3.0
4.0
5.0
6.0
(M/S)
5
10
20
30
40
50
(mm)
0.025
0.033
0.050
0.075
0.100
0.150
(ft)
DISTANCE FROM DUMMY SAMPLE PLATE

Figure 9. - Dried-up samples in plastic boxes.

Figure 10. - Clay samples in submerged storage.

Figure 11. - Layer of mushy clay stuck to bottom of plastic handling box.

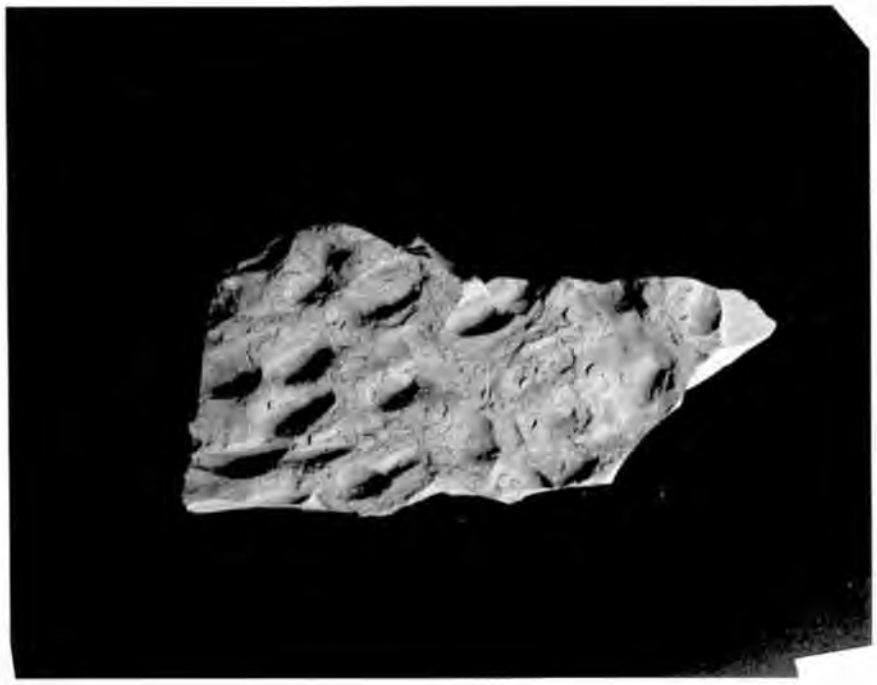

(a) Flow sculptured dimples at intermediate development stage. Dark shadows are inside bottoms of dimples.

(b) Underside of same piece showing thin lamina of leaner sandy clay adjacent to fatter clay lamina.

Figure 12. - Views of sample showing dimples and lamina.

(a) A piece of open jointed river flow surface showing typical mature flow sculpturing.

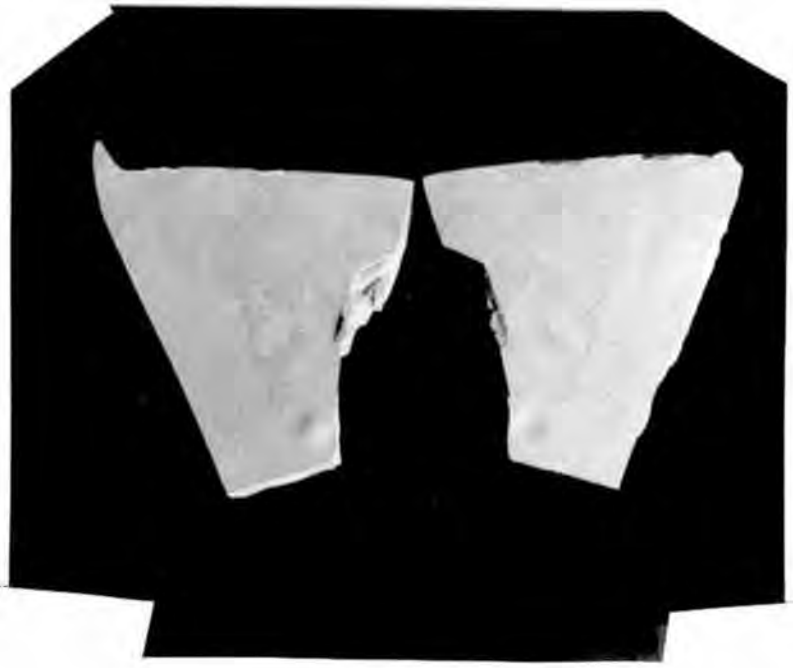

(b) Inside of same piece parted showing an interface of silty and clayey layers. The depression in the upper part is a cast of the mound formed over a piece of gravel under the mound.

Figure 13. - Views of sample pieces showing flow sculpturing and interface.

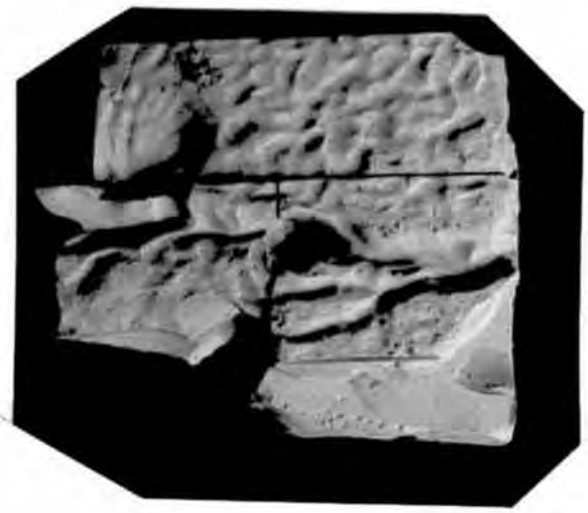

(a) Flow surface with kidney shaped scour hole caused by a 10-mm (3/8-in) pebble scoured out of the clay.

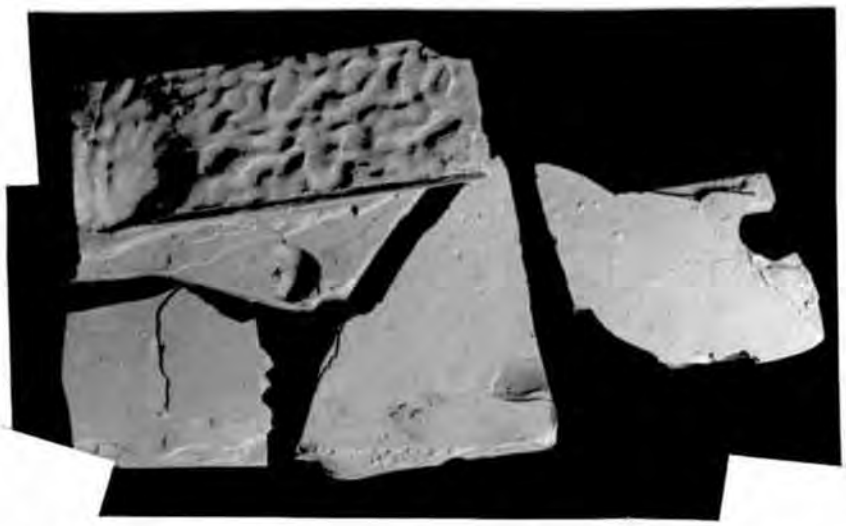

(b) Same piece opened showing section through kidney-shaped scour hole.

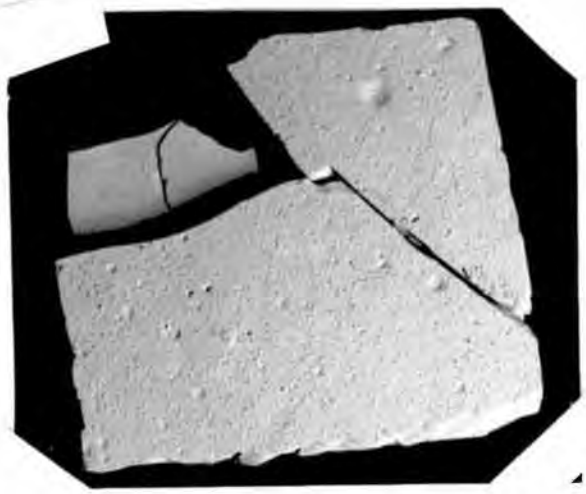

(c) Underside showing sparse sand probably deposited from floating and melting glacier ice.

Figure 14. - Views of sample showing scour and sand deposits.

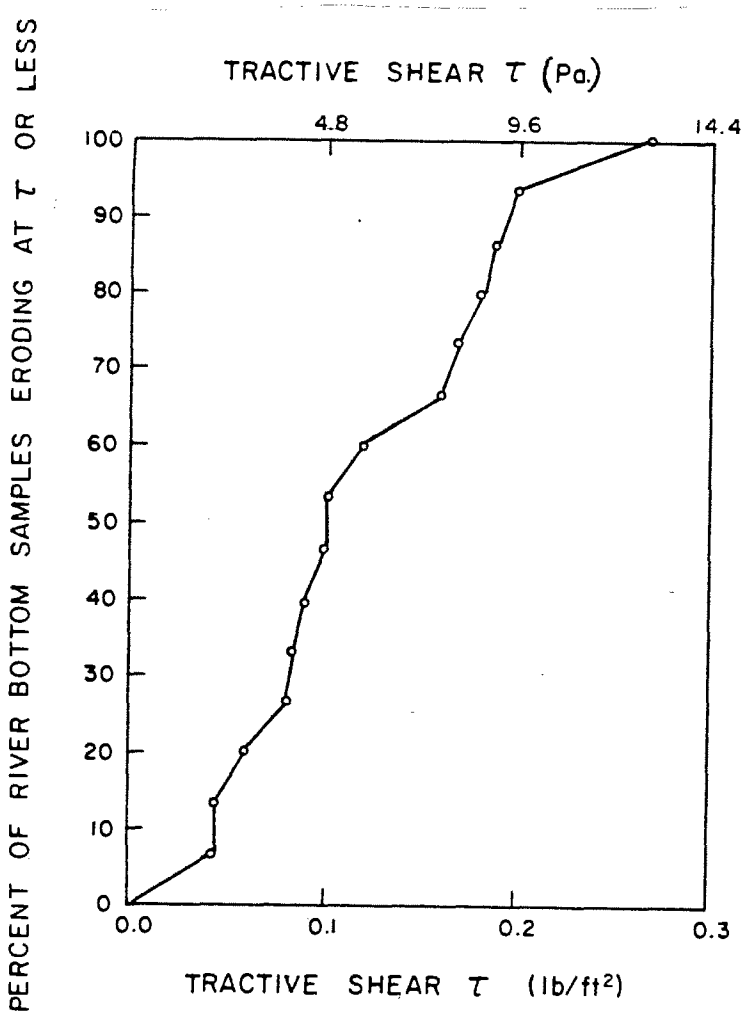

Figure 15. - Cumulative distribution of tractive shear values for first noted erosion on samples.

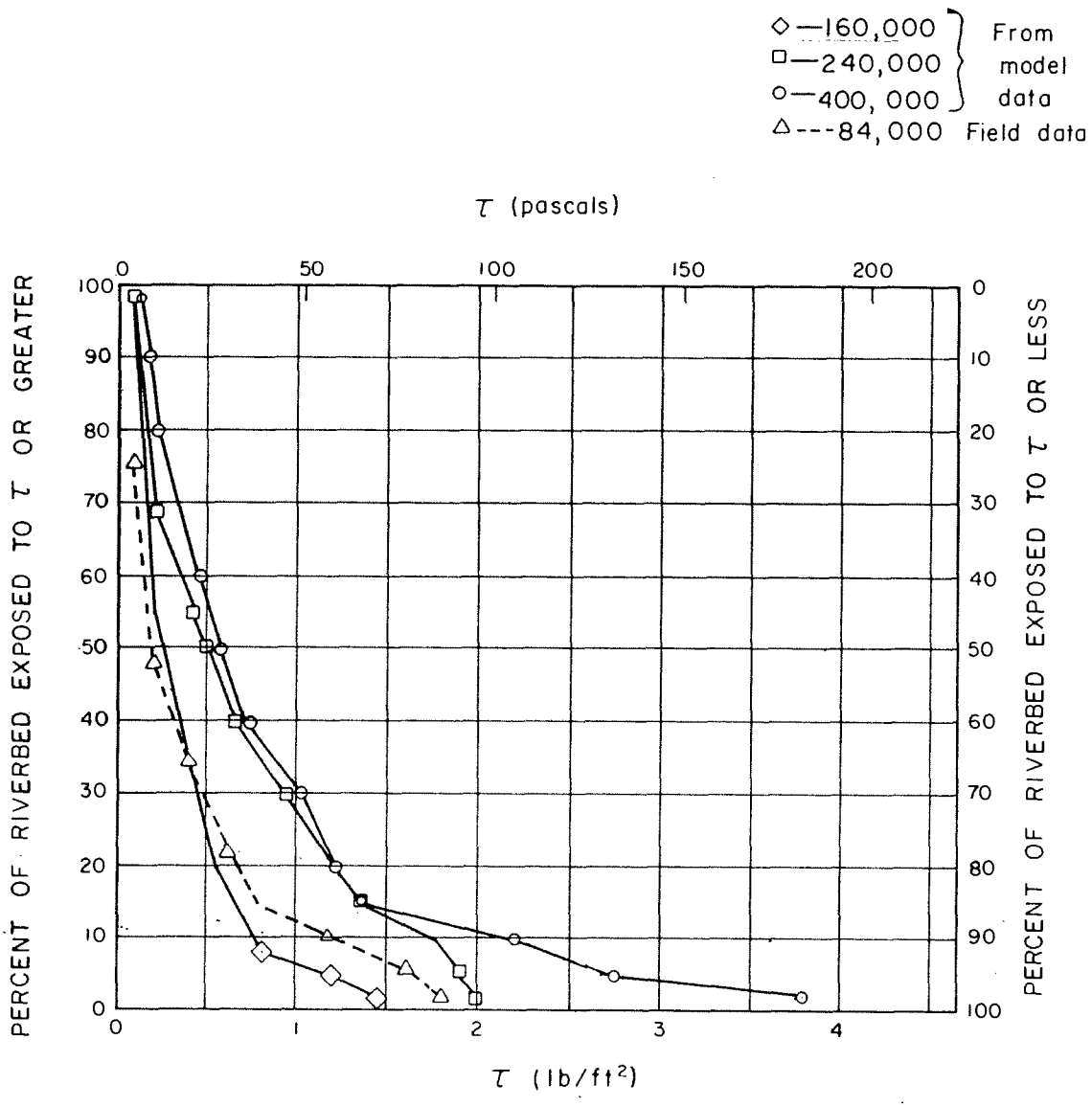

Figure 16. - Cumulative distribution of tractive shear values on river bottom for various discharges.

Figure 17. - Gessler's transport function. [10]

V_{tl} = Velocity at threshold of sediment motion for flow over level bed
V_{ts} = Velocity at threshold of sediment motion for flow over sloped bed
Z = Horizontal component of bed slope
τ_{tl} = Tractive shear at threshold of sediment motion for flow over level bed
τ_{ts} = Tractive shear at threshold of sediment motion for flow over sloped bed
θ = Angle of repose for bank material
φ = Slope angle of embankment

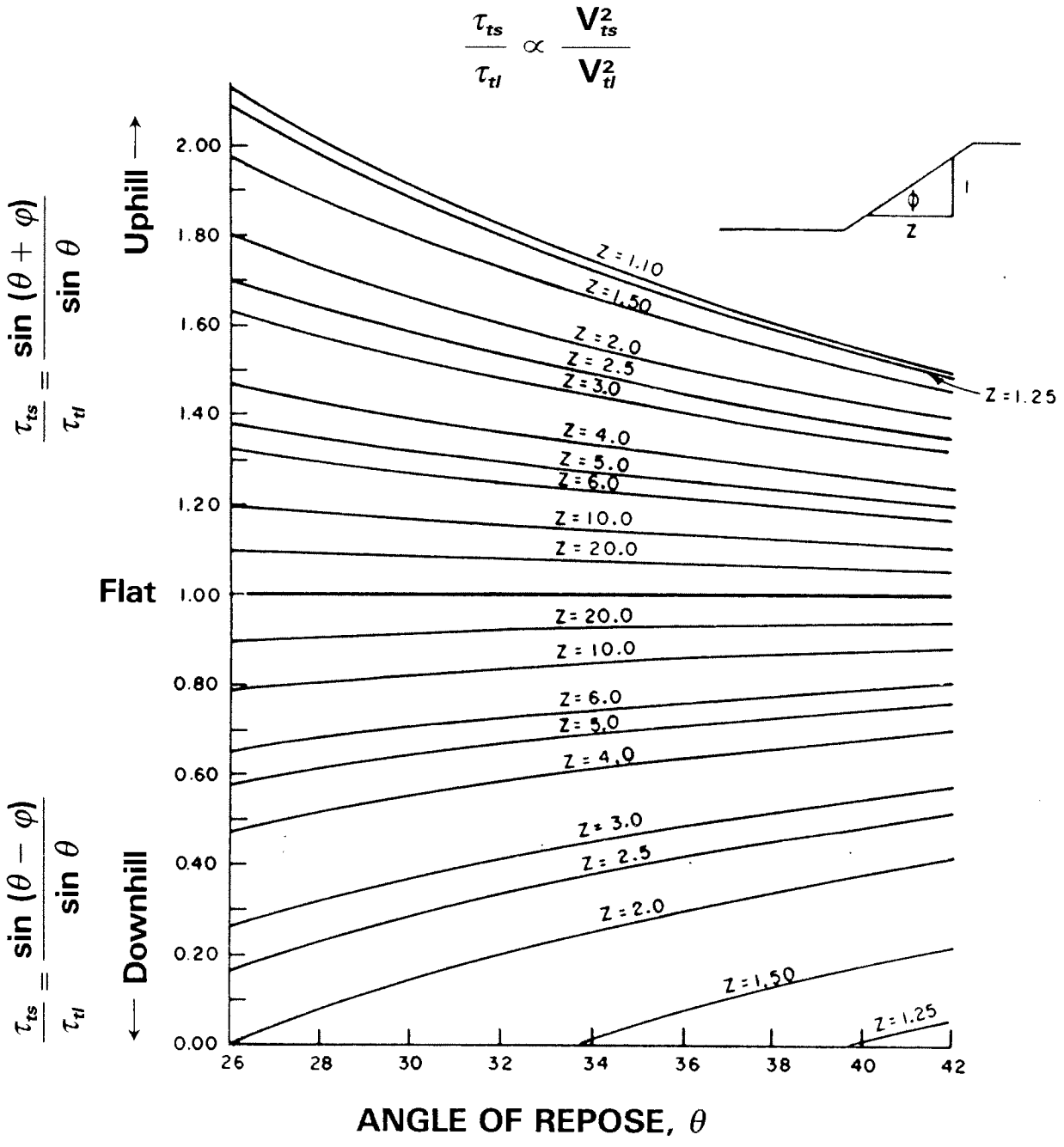

Figure 6. – Embankment stability correction factor for slope gravity effect during uphill and downhill flow.

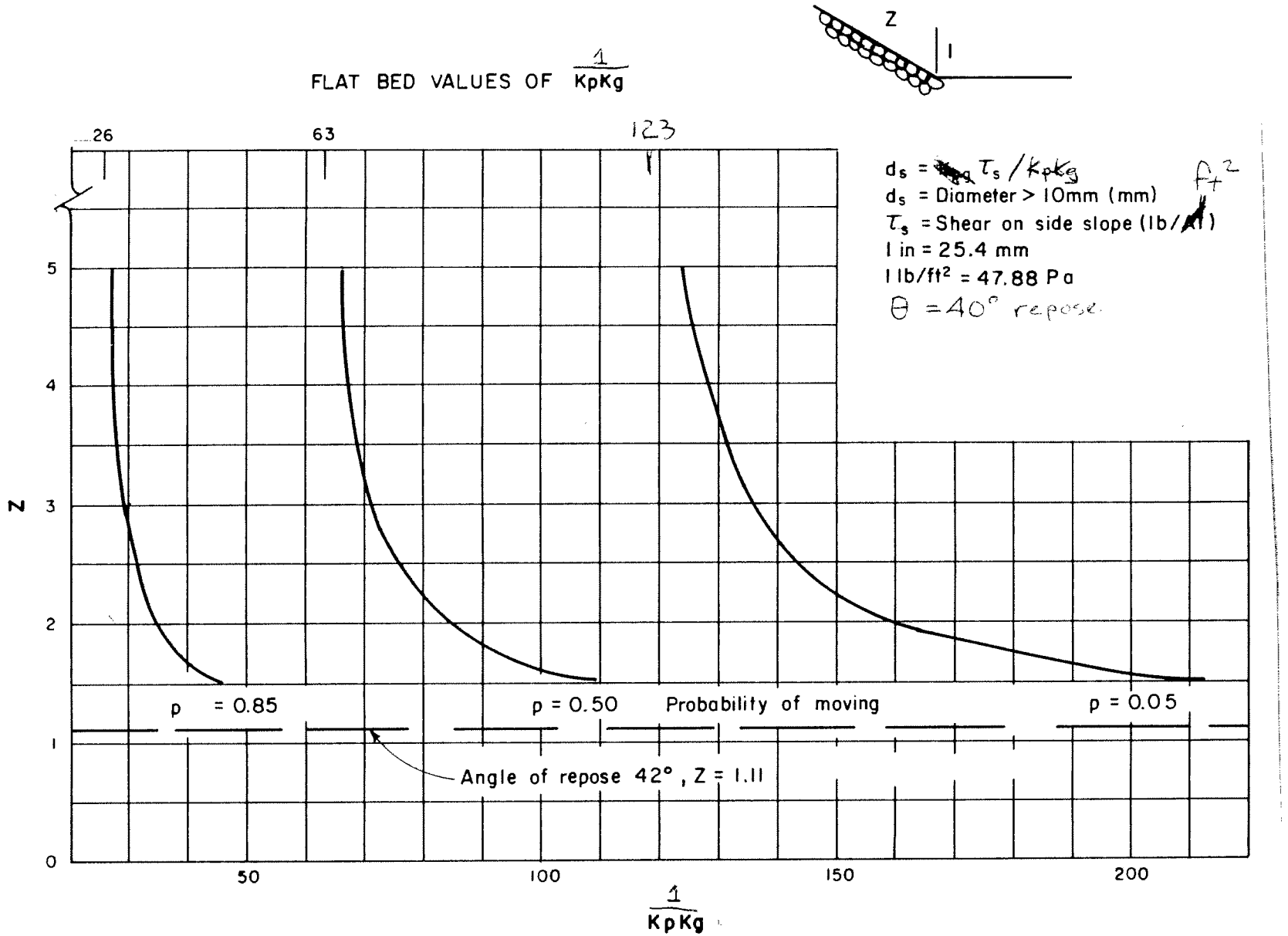

Figure 18. - Design curves for protective gravel blankets on side slopes.

APPENDIX

Preliminary results of clay erosion tests
Gradation tests

APPENDIX

Preliminary results of clay erosion tests
Gradation tests

CLAY BLOCK SAMPLES*

Site No. 1 at station 105+00 - left blank

Sample No. 1 - Varved, some discontinuous vertical joints, some silt partings, horizontal bedding

Sample No. 2 - Varved, some discontinuous vertical joints, gently dipping 2 to 5° downstream.

Sample No. 3 - Thin bedded to varved, 45° joint dipping into the bank (west), 2 to 5° dipping downstream

Sample No. 4 - Varved, horizontal bedding, no joints visible

Sample No. 5 - Varved, no joints visible, 2 to 5° dipping downstream

Clay very firm in saw cut exposures; can be separated along bedding and silt partings with light to moderate knife pressure.

Occasional interbed to 1 to 2 inches.

Joints widely spaced - chiefly greater than 5 feet, but locally to several inches.

Bedding attitude from horizontal to 5° dip to northwest or downstream.

Site No. 2 at station 167+00 - right bank

Sample No. 6 - Thin bedded clay with 2- to 3-inch-thick bed of sandy silt; bedding dips 15 to 20° into the bank (east); sandy silt bed firm but friable with moderate finger pressure; some sharply dipping joints - hairline open

Sample No. 7 - Medium to thick bedded; 1 to 4 inches; bedding dips 5 to 10° into bank (east); some vertical and steeply dipping joints - open joints spaced 3 to 8 inches

Sample No. 8 - Appear to be thick bedded; greater than 4 inches; bedding dips 5 to 10° into bank (east)

Clay exposure disturbed from slide movement.

Bedding somewhat contorted and joints chiefly open (hairline). Also much irregular fracturing in exposures.

*Typed from preliminary handwritten notes by Brent Carter, Regional Geologist.

SAMPLE NO. 1 (marked No. 2 on the stock tank)

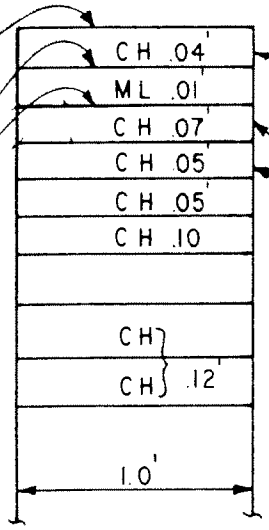

Trace of sand and small gravels (angular to subangular)

Trace of silt on parting planes between CH layers

Laminated ML, CL, CH (each bed ≈ 0.06 inch thick)

All three surfaces tested had mold and cast structures from sand and gravel grains.

Flow

Planar view

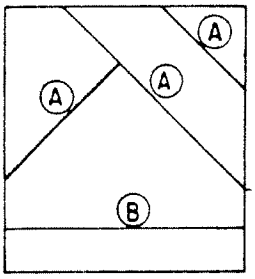

Sample surface prior to first run

A. Joints, discontinuous, were probably in the sample before disturbing, but not open, no staining on joint surfaces.

B. Joint, discontinuous, staining (black) one-eighth inch deep.

CH = fat clay - green
CL = lean clay - green (lighter than CH)
ML = lean silt - green to light brown

SAMPLE NO. 2 (sample had No. 2 scribed in it, but was marked No. 1 on stock tank)

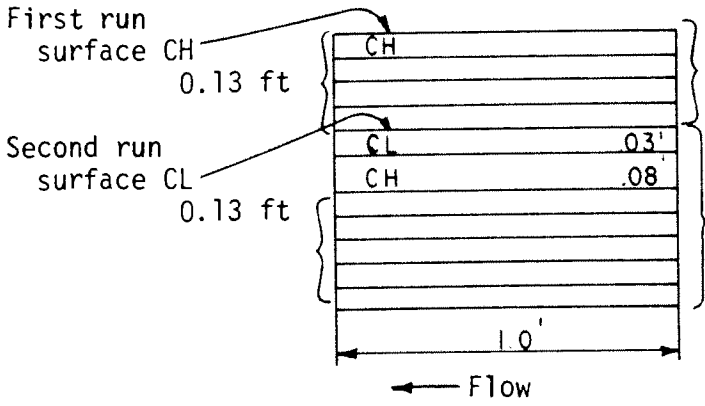

Laminated CH, CL, ML, individual lamina paper thin to 0.02 ft

Laminated CH, CL, ML, individual lamina paper thin to 0.08 ft thick

80 percent of lamina are CH, 15 percent are CL, 5 percent ML

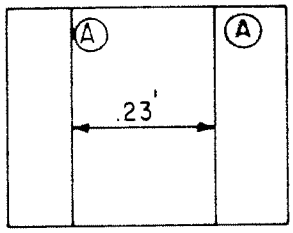

Planar view

A. Joints discontinuous, staining (black) one-half inch deep. Open joint. Vertical joints

CH = fat clay - green
CL = lean clay - green (lighter than CH)
ML = lean silt - green to light brown

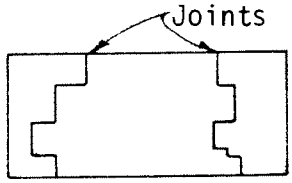

Schematic (not to scale)

When this sample was run, the jointing developed a stairstep pattern.

SAMPLE NO. 3

Run No. 1
surface CH

Run No. 2
surface CH

Run No. 3
surface ML

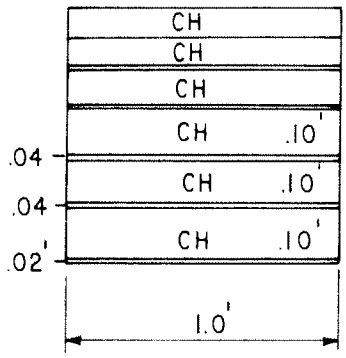

ML

ML to ML-CL

Laminated CH, ML-CL, ML individual lamina 0.01 to 0.10 feet thick. Parting planes have trace of silt and/or very fine micaceous sand.

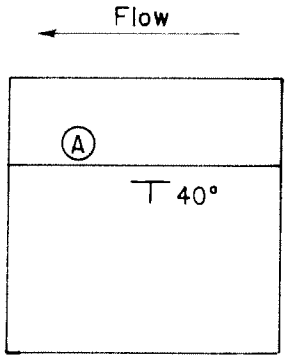

A. Joint, continuous, dips into bank at 40°.

Planar view

CH = fat clay - green to dark grey

ML to ML-CL = lean silt to clayey silt - green (lighter than CH)

SAMPLE NO. 4

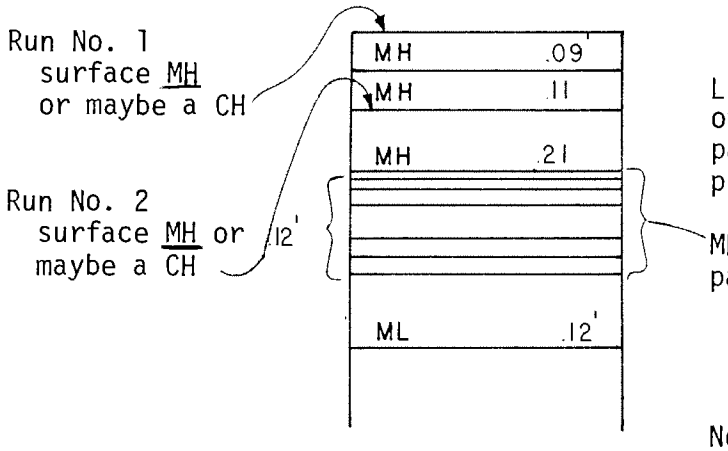

Laminated MH and ML, lower part of sample was mostly an ML. This part was shaved off during sample preparation.

MH, ML individual lamina from paper thin to 0.01 foot.

No noticeable joints

MH = elastic silt - grey-green
ML = lean silt - green

SAMPLE NO. 5

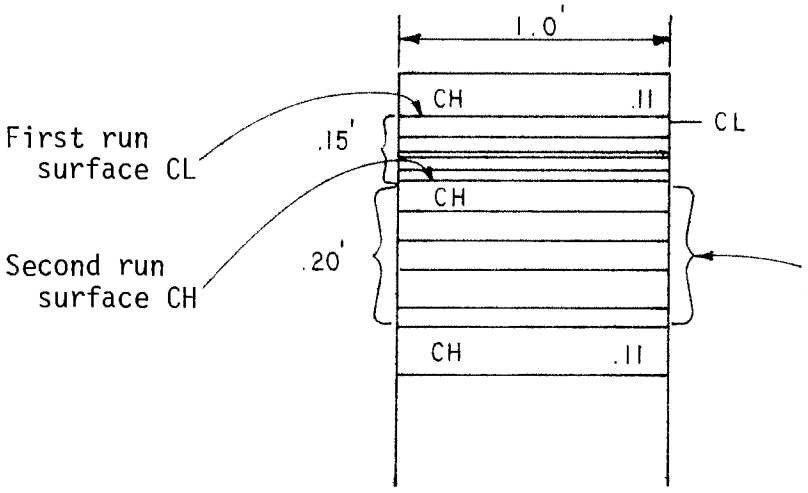

Laminated beds, paper thin to 0.05 foot. 85 percent of lamina are CH, 15 percent CL, trace of ML (dusting) on parting planes.

CH = fat clay - green to dark grey
CL = lean silt - green

The CL surface of run No. 1 was smooth with a fine dusting of silt, when this surface eroded off (in layers one-eighth to three-sixteenths inch thick). The parting surface exposed had pods of what seemed to be ash, approximately two per square inch, grey.

The CH surface of run No. 2 had several grains/rock fragments. <2 mm diameter, approximately five per square inch.

SAMPLE NO. 6

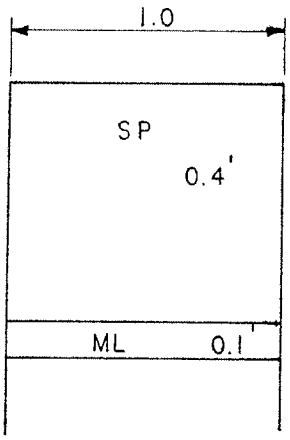

No erosion test run.
Sample fell apart when it was removed from the Plexiglass container.

Sample was very disturbed and broken. Fine to medium grained sand approximately 15-20 percent silt. SP brown.

SAMPLE NO. 7

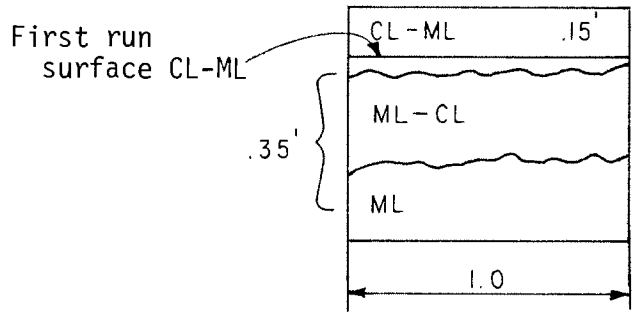

Gradational, sample grades from a silty clay down to a lean silt. Appears massive, no distinct individual beds.

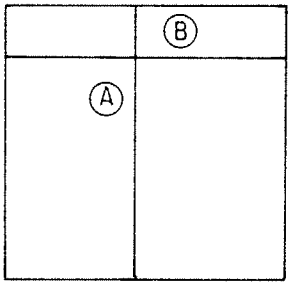

Planar view

A. Joint, continuous through sample, possible movement along this joint, materials on opposite sides of joint seem to have subtle differences in texture and physical characteristics. Vertical joint.

B. Joint, vertical, continuous

CL-ML = silty clay
ML-CL = clayey silt
ML = silt

greenish grey

SAMPLE NO. 8

First run
surface ML-CL
(natural surface)

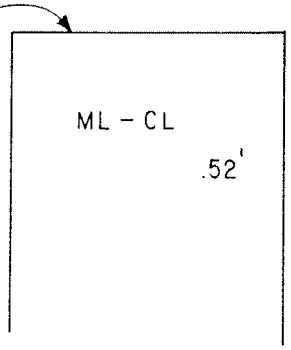

Massive clayey silt, no distinct individual beds, no visible joints, greenish grey

7-1415 (8-70)
Bureau of Reclamation

GRADATION TEST

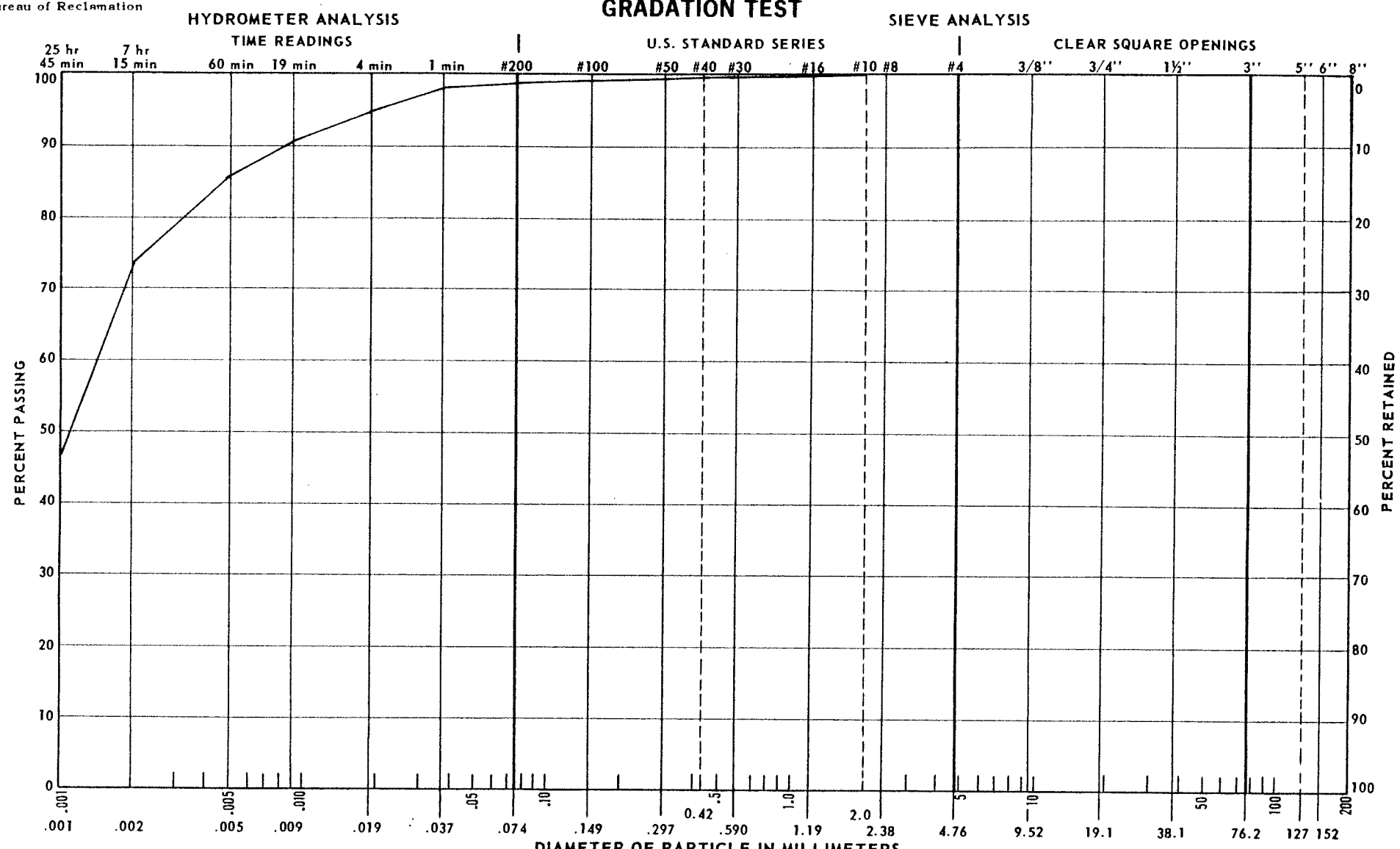

FINES	SAND			GRAVEL		COBBLES
	FINE	MEDIUM	COARSE	FINE	COARSE	

CLASSIFICATION SYMBOL MH

Gravel 0 %
Sand 0.8 %
Fines 99.2 %

ATTERBERG LIMITS
Liquid Limit 70.4 %
Plasticity Index 34.5 %
Shrinkage Limit ____ %

SPECIFIC GRAVITY
Minus No. 4 ____
Plus No. 4
Bulk ____ Apparent ____

NOTES
MOISTURE CONTENT 40.3 %

SAMPLE NO. #1 CLAY EROSION TEST HOLE NO. ____ DEPTH ____ ft (____ m)

FIGURE

GPO 832-939

7-1415 (8-70)
Bureau of Reclamation

GRADATION TEST

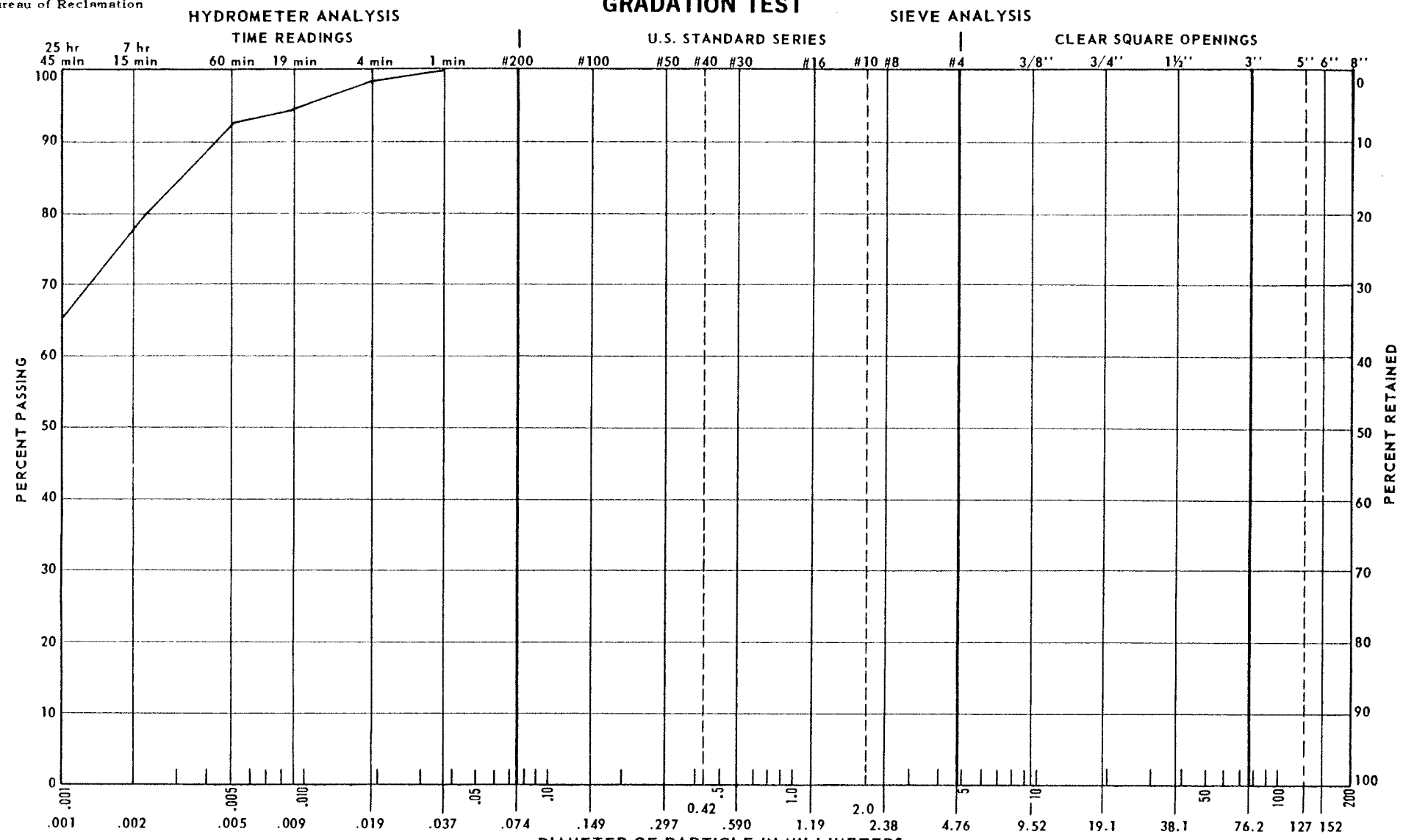

CLASSIFICATION SYMBOL MH

Gravel 0 %

Sand 0 %

Fines 100 %

ATTERBERG LIMITS

Liquid Limit 78.5 %

Plasticity Index 42.5 %

Shrinkage Limit ____ %

SPECIFIC GRAVITY

Minus No. 4 ____

Plus No. 4

Bulk ____ Apparent ____

NOTES MOISTURE CONTENT 41.1%

SAMPLE NO. #2 CLAY EROSION TEST HOLE NO. ____ DEPTH ____ ft (____ m)

FIGURE

GPO 832-939

7-1415 (8-70)
Bureau of Reclamation

GRADATION TEST

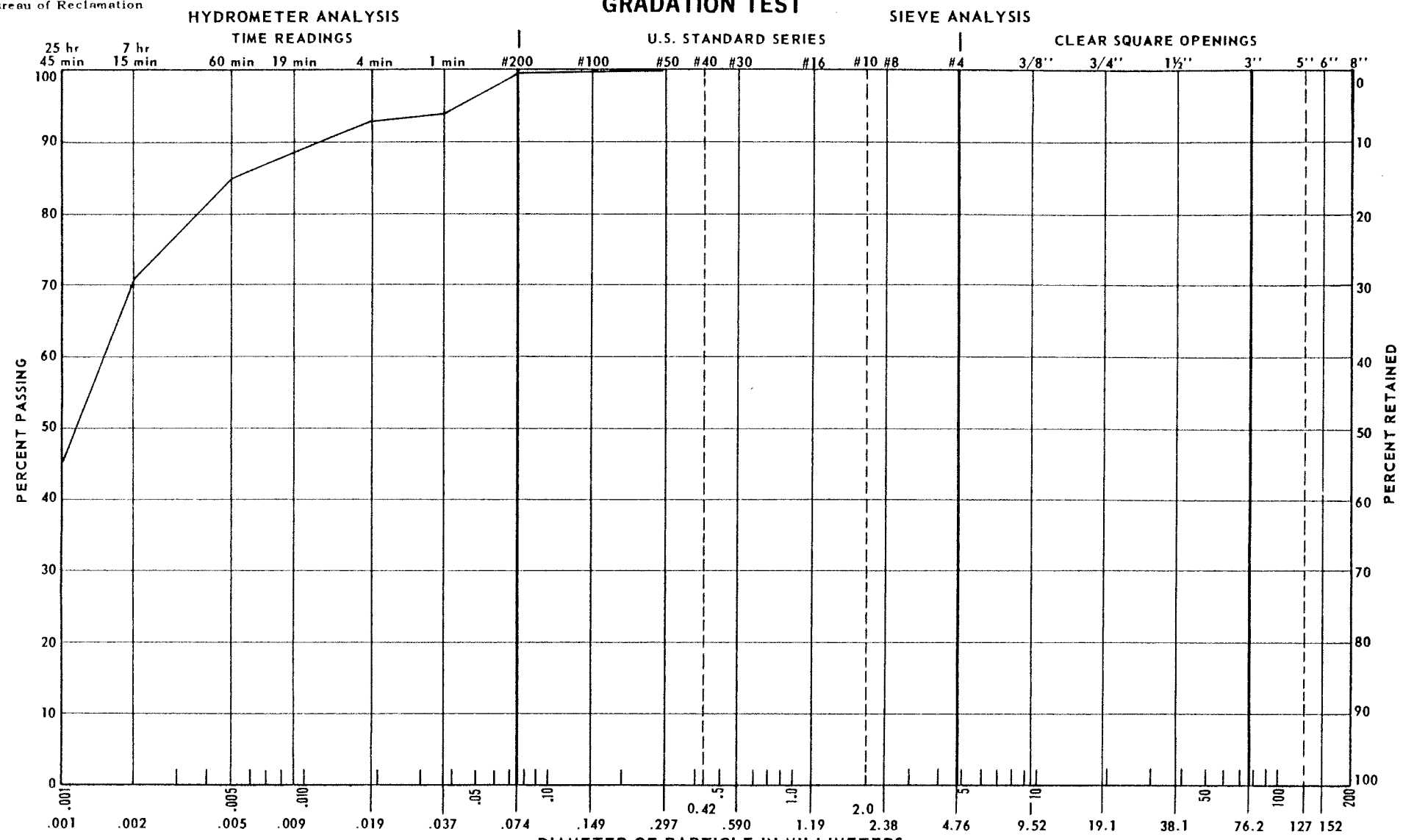

CLASSIFICATION SYMBOL CH

Gravel 0 %

Sand 0.2 %

Fines 99.8 %

ATTERBERG LIMITS

Liquid Limit 75.3 %

Plasticity Index 39.1 %

Shrinkage Limit ____ %

SPECIFIC GRAVITY

Minus No. 4 ____

Plus No. 4

Bulk ____ Apparent ____

NOTES

MOISTURE CONTENT 40.1

SAMPLE NO. 3 CLAY EROSION TEST HOLE NO. ____ DEPTH ____ ft (____ m)

FIGURE

GPO 832-939

7-1415 (8-70)
Bureau of Reclamation

GRADATION TEST

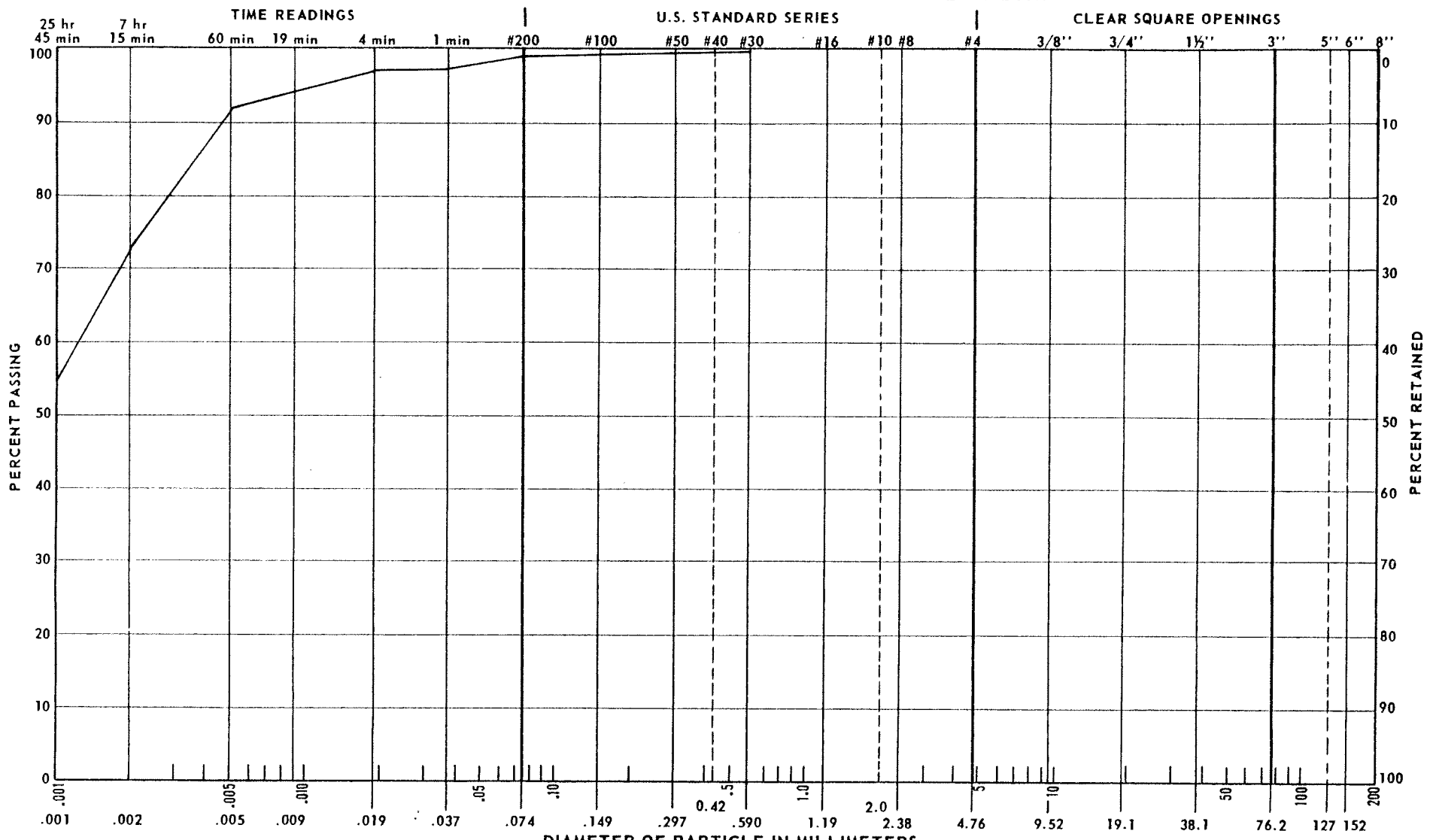

CLASSIFICATION SYMBOL CH

Gravel 0 %

Sand 0.2 %

Fines 99.8 %

ATTERBERG LIMITS

Liquid Limit 59.3 %

Plasticity Index 29.8 %

Shrinkage Limit _____ %

SPECIFIC GRAVITY

Minus No. 4 _____

Plus No. 4

Bulk _____ Apparent _____

NOTES

MOISTURE CONTENT 35.4

SAMPLE NO. #4 CLAY EROSION TEST HOLE NO. _____ DEPTH _____ ft (_____ m)

FIGURE

GPO 832 - 939

7-1415 (8-70)
Bureau of Reclamation

GRADATION TEST

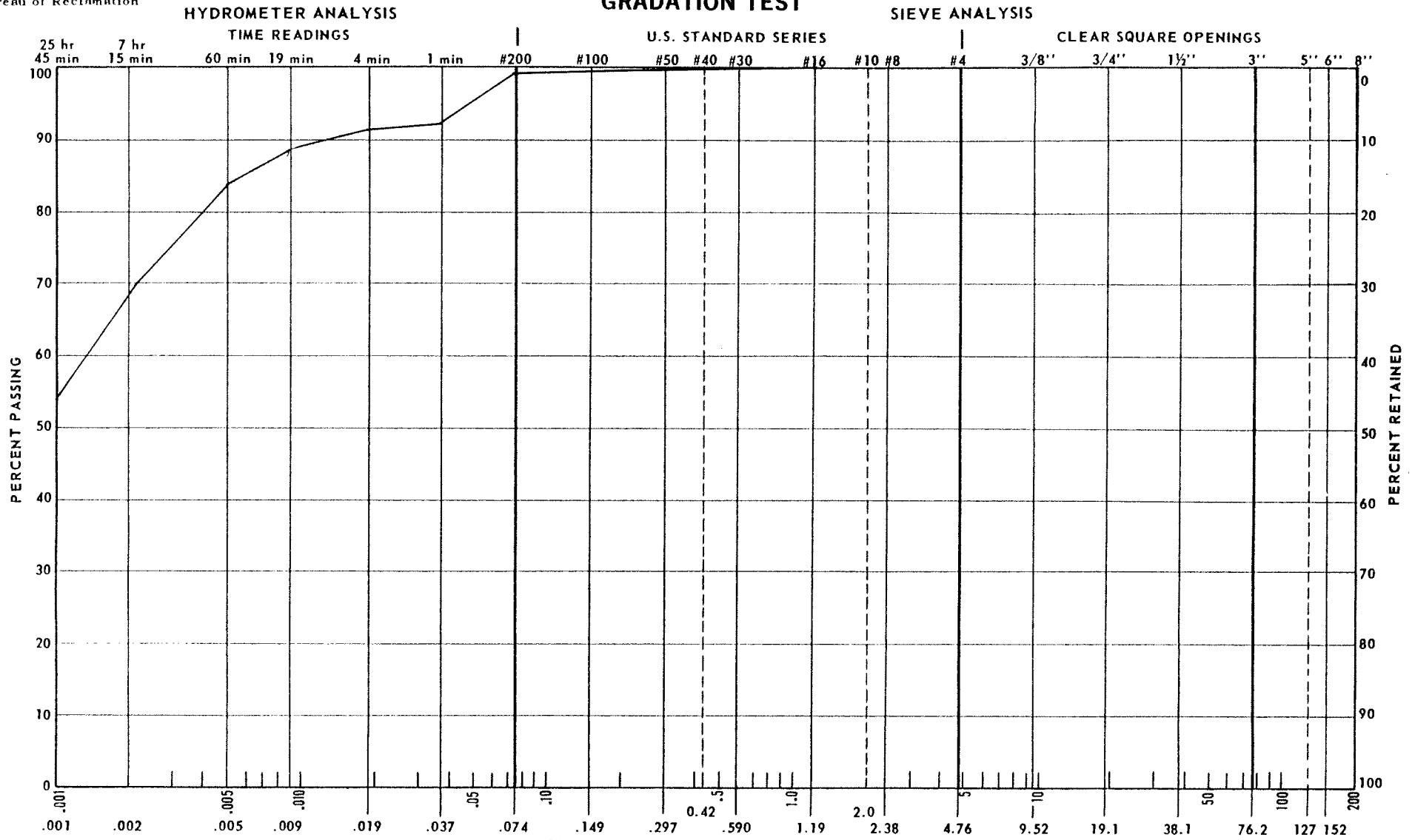

CLASSIFICATION SYMBOL CH

Gravel 0 %
Sand 0.2 %
Fines 99.8 %

ATTERBERG LIMITS
Liquid Limit 77.4 %
Plasticity Index 43.7 %
Shrinkage Limit ____ %

SPECIFIC GRAVITY
Minus No. 4 ____
Plus No. 4
Bulk ____ Apparent ____

NOTES
MOISTURE CONTENT 39.1

SAMPLE NO. #5 CLAY EROSION TEST HOLE NO. ____ DEPTH ____ ft (____ m)

FIGURE

GPO 832-939

7-1415 (8-70)
Bureau of Reclamation

GRADATION TEST

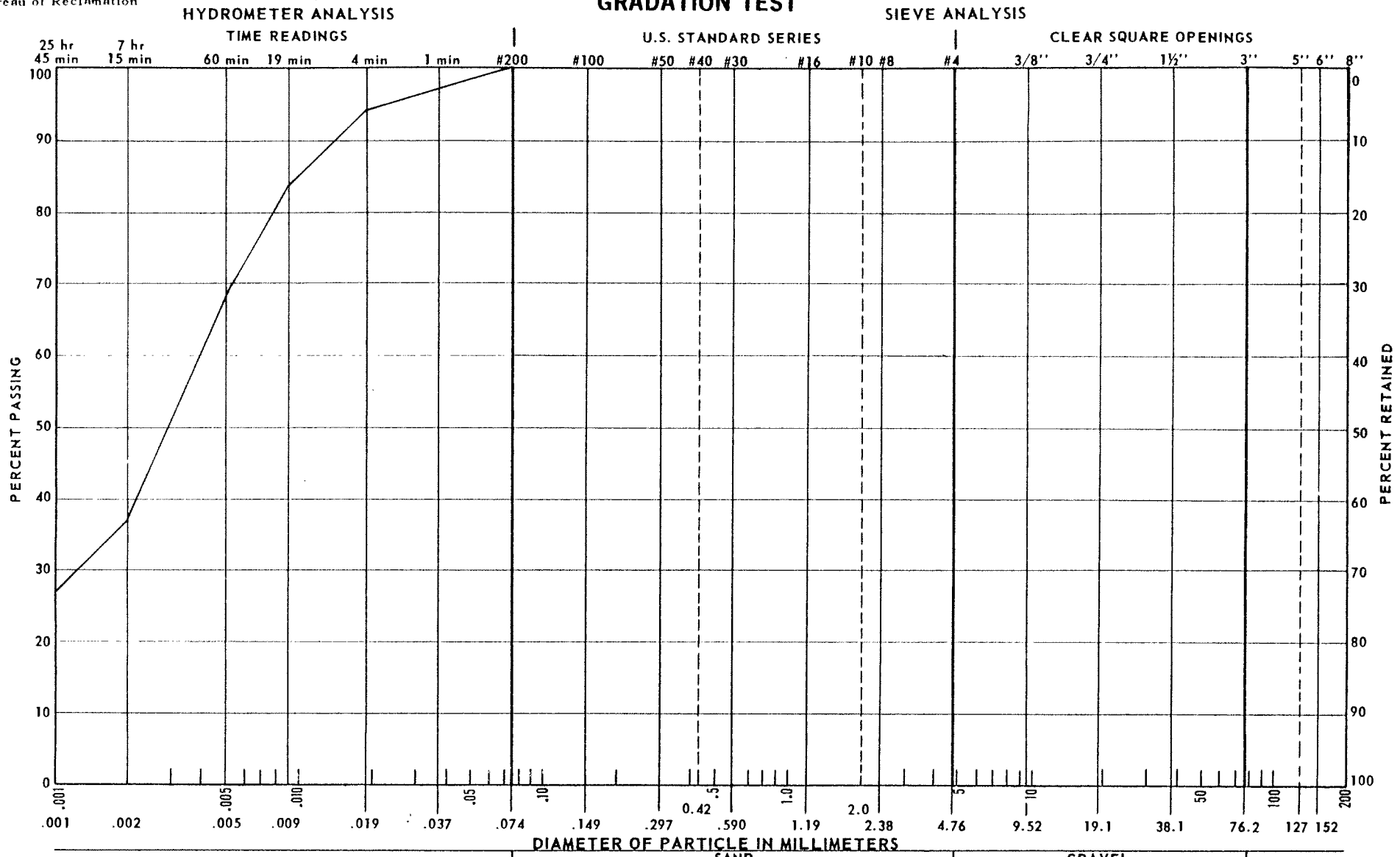

FINES	SAND			GRAVEL		COBBLES
	FINE	MEDIUM	COARSE	FINE	COARSE	

CLASSIFICATION SYMBOL _____

Gravel 0 %

Sand 0 %

Fines 100.0 %

ATTERBERG LIMITS

Liquid Limit _____ %

Plasticity Index _____ %

Shrinkage Limit _____ %

SPECIFIC GRAVITY

Minus No. 4 _____

Plus No. 4

Bulk _____ Apparent _____

NOTES

MOISTURE CONTENT 31.5

SAMPLE NO. 7 CLAY EROSION TEST (UPSTREAM SIDE) DEPTH _____ ft (_____ m)

FIGURE

GPO 832-939

7-1415 (8-70)
Bureau of Reclamation

GRADATION TEST

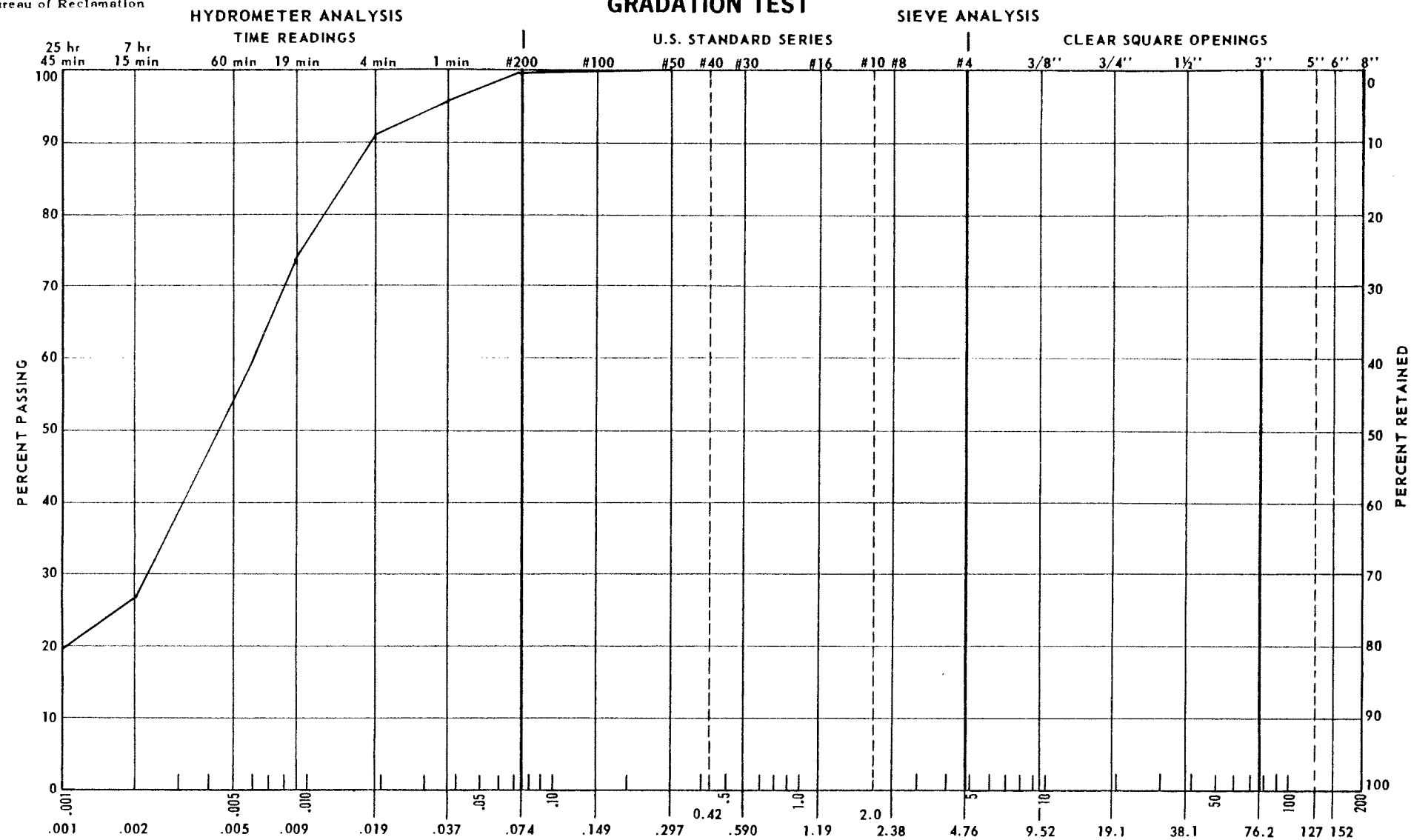

FINES	SAND			GRAVEL		COBBLES
	FINE	MEDIUM	COARSE	FINE	COARSE	

CLASSIFICATION SYMBOL _____

Gravel 0 %

Sand 0.1 %

Fines 99.9 %

ATTERBERG LIMITS

Liquid Limit _____ %

Plasticity Index _____ %

Shrinkage Limit _____ %

SPECIFIC GRAVITY

Minus No. 4 _____

Plus No. 4

Bulk _____ Apparent _____

NOTES

MOISTURE CONTENT 30.0

SAMPLE NO. 7A CLAY EROSION TEST (D/S SIDE) HOLE NO. _____ DEPTH _____ ft (_____ m)

FIGURE

GPO 832-939

7-1415 (8-70)
Bureau of Reclamation

GRADATION TEST

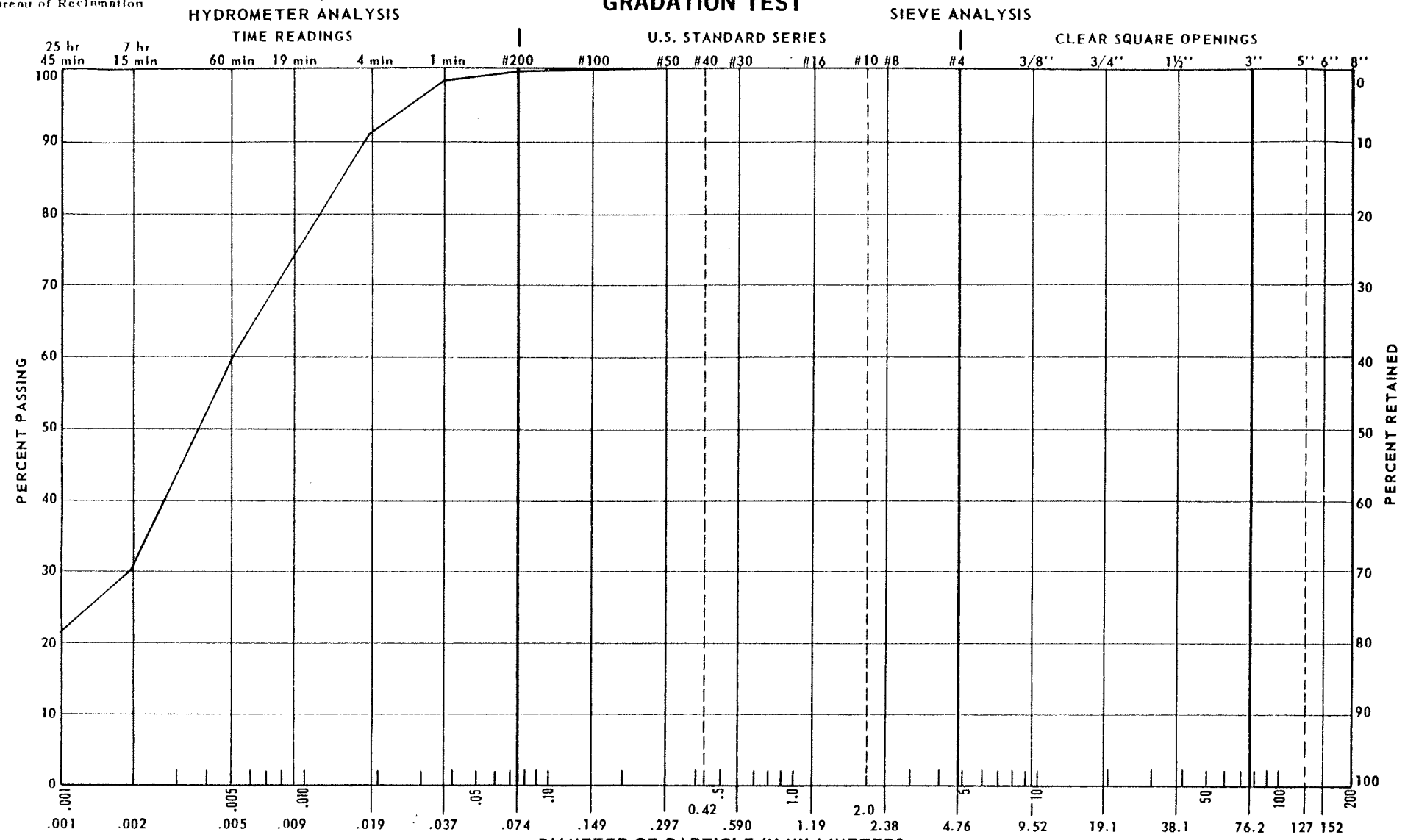

CLASSIFICATION SYMBOL ML

Gravel 0 %

Sand 0.2 %

Fines 99.8 %

ATTERBERG LIMITS

Liquid Limit 36.0 %

Plasticity Index 11.1 %

Shrinkage Limit ____ %

SPECIFIC GRAVITY

Minus No. 4 ____

Plus No. 4

Bulk ____ Apparent ____

NOTES

MOISTURE CONTENT 57.0

SAMPLE NO. #8 CLAY EROSION TEST HOLE NO. ____ DEPTH ____ ft (____ m)

FIGURE

GPO 832-939